GULF GENERAL ATOMIC

Gulf-GA-A10988

A REVIEW OF HIGH-TEMPERATURE GRAPHITE IRRADIATION BEHAVIOR

by

G. B. Engle and W. P. Eatherly*

*Present Address: Oak Ridge National Laboratory, P.O. Box X, Oak Ridge, Tennessee 37830

Gulf General Atomic Project 271

March 1972

GULF GENERAL ATOMIC COMPANY
P.O. BOX 608, SAN DIEGO, CALIFORNIA 92112

May 5, 1972

DISCLAIMER

ABSTRACT

The irradiation behavior of reactor graphites at high temperatures (500° to 1400°C) to high fluences (up to 4 x 10^{22} n/cm^2) is reviewed. Recent data generated during the period 1965 through 1971 are emphasized. The review covers graphite manufacture, irradiation damage, dimensional and structural changes, thermal expansion, thermal conductivity, Young's modulus, strength, and irradiation-induced creep.

Graphite-moderated reactors utilize graphites manufactured with conventional binder-filler technology or some new nonconventional methods. In the binder-filler method of manufacture fillers can range from natural flakes or needle-coke, which are extremely anisotropic, to Gilsocoke, proprietary isotropic cokes, and carbon blacks which are extremely isotropic. Other nonconventional methods, some of them proprietary, have been used to produce high-density, high-strength graphites. These materials are more uniform in microstructure and the traditional binder-filler interfaces are not visible.

Irradiation effects in single crystals, annealed pyrolytic carbons, as-deposited pyrolytic carbons, and highly oriented graphites are discussed where the data relate to the interpretation of the behavior of reactor graphites.

Irradiation damage in single crystals and annealed pyrolytic carbons has been studied at temperatures up to 1350°C to high fluences. Interstitial migration in the c-axis direction has been postulated and large interstitial loops have been observed in twist boundaries of annealed pyrolytic carbons. Examination of reactor graphites has been attempted, but the results have not been highly successful due to experimental difficulties dealing with the complex nature of the microstructure of these materials. Speculations that observations on the more perfect crystals may hold for the reactor graphites lead to the conclusions that c-axis diffusion may occur at lower temperatures in reactor materials. An increase in the crystalline perfection improves the dimensional stability of the crystallites.

Graphite data are assembled to show dimensional changes in the range 400° to 1300°C to fluences of up to 4×10^{22} n/cm^2 (E > 0.050 MeV) for anisotropic and near-isotropic binder-filler graphites and nonconventional high-density, high-strength materials.

There appears to be almost unanimous agreement among the various investigators that volume expansion after turnaround at high temperatures results from pore generation and that isotropic graphites with relatively high density and high strength are the most stable. These materials usually have relatively small crystallites, but their high strength and isotropy offset the crystallite size effect and prevent pore generation, which is responsible for the large volume expansions observed in the weaker more anisotropic graphites. Again there is good agreement in that the lower pore generation results from a higher irradiation-induced creep rate in the isotropic materials that

allows plastic deformation to relieve stresses. Pyrolytic carbons behave in a like manner.

Dimensional instability appears to be maximized in the range 900° to 1200°C due to high expansion rates. However, some data are available to indicate that above 1200°C the expansion rate decreases again. More work is needed to confirm this observation.

Some progress has been made in explaining the microstructural and porosity changes that occur at high temperatures and hig fluences, but the complexity of reactor graphite structures permits only a qualitative interpretation at present. Certain relatively large pores or cracks close during densification due to c-axis expansion, while other micropores are generated within or between crystallites. Macroporosity is generated when volumetric expansion begins. Lack of quantitative methods to analyze pore morphology and structure after irradiation continues to slow progress in this area.

Early models based on thermal expansion and crystallite orientation were successful in predicting dimensional changes at low fluences, but are of limited value at high fluences. These models have been updated to conform to recent data obtained at high temperatures and higher fluences but microstructural and porosity changes continue to complicate the efforts to produce a quantitative model.

Limited data are available on conventional binder-filler graphites that attempt to correlate dimensional changes with variations of certain fabrication

processes. These studies show the dimensional changes to be sensitive to manipulation of the binder-coke content.

Thermal expansivity changes in reactor graphites during high-temperature irradiation correspond with the onset of volumetric expansion. Thermal expansivity changes are not uniform among the graphites; the weak, anisotropic materials with initially low coefficients increase whereas the strong, isotropic graphites with initially high coefficients decrease. No theoretical analysis has been undertaken to explain the thermal expansion changes. It had generally been assumed that thermal expansivity would increase after basal plane cracks, which accommodate c-axis expansion, were exhausted. This idea may have to be revised in light of the current data.

Thermal conductivity degrades rapidly at low fluences; the magnitude of the fractional changes decreases with increasing irradiation temperature. Analysis of the thermal conductivity changes in terms of structural damage that causes dimensional changes revealed that submicroscopic clusters, vacancies, and vacancy loops are responsible for thermal conductivity changes while interstitial loops and collapsed vacancy lines which cause dimensional changes are insignificant. At high fluences after large volume changes have occurred there is a further catastrophic reduction in thermal conductivity which appears to be associated with the disintegration of the structure.

The mean tensile strength was observed to increase in graphites after irradiation at 1200°C, but the probability of failure at some stress below the mean fracture stress was higher for graphites with initially higher mean

strengths. This was interpreted to mean that variations of the mean strength are not indicative of the actual risk of failure.

Young's modulus increases rapidly at low fluences and quickly saturates. It is generally accepted that the increase is due to pinning of dislocations by irradiation-induced defects, and the saturated value represents complete pinning.

Irradiation-induced creep constants have been measured at temperatures up to 1200°C. In an irradiation field graphites will withstand strains ten times that of unirradiated samples before fracture occurs.

1. INTRODUCTION

Artificial graphite was used as the neutron moderator and reflector for the first atomic pile at the University of Chicago. Later it was chosen for the production reactors at the Hanford Works, Richland, Washington (Nightingale, 1962), and a variety of research and test reactors scattered around the world. In these early reactors the graphite operated from room temperature to about 700°C. In the early 1950s graphite-moderated gas-cooled reactors were developed in the United Kingdom, with carbon dioxide as the coolant. In this reactor concept the graphite remained well below its oxidizing temperature to maintain compatibility with the carbon dioxide. These reactors, termed Calder Hall Class Reactors, were followed by an advanced design also cooled with carbon dioxide, known as the Advanced Gas-Cooled Reactor (AGR). During this same period the Russians were developing graphite-moderated pressurized-water power reactors (Petrosyants, 1969).

In the 1950s the concept of the high-temperature gas-cooled reactor was introduced with helium as the coolant. In these designs the temperature of the fuel, rather than that of the graphite, limits the operating temperature. Concurrent development of carbon-coated refractory fuel particles has permitted design temperatures of 1000° to 1300°C and lifetime fluences of 5 to 10×10^{21} n/cm^2. The most notable among the helium-cooled reactor projects

by high-energy neutrons. The magnitude of these changes is dependent not only on the operational temperature and total neutron fluence but also on the microstructure of the particular graphite.

During the period from the early 1940s through 1960, a considerable amount of irradiation data was obtained and voluminous studies were completed by the General Electric Company at its Hanford Atomic Products Operation. These data were obtained primarily from irradiation experiments in the various Hanford Graphite Reactors at 30° to 700°C. The experiments provided extensive data on dimensional changes, stored energy release, structural deterioration, and physical and mechanical property changes. The work was summarized in Nuclear Graphite (Nightingale, 1962), which includes chapters on general graphite technology and properties in addition to a review of the existing irradiation data.

As reactor design requirements reached toward higher temperatures and fluences during the 1960s, a number of books and reviews kept pace with the expanding technology. Notable among these are Simmons (1962) and Reynolds (1968). Articles on nuclear carbon and graphite technology, irradiation data, and theory have also appeared in various sections of the series Chemistry and Physics of Carbon (Walker, 1966, 1969). Included in this series were articles by Reynolds (1966) on physical properties of graphite, Bokros (1969) on pyrolytic carbons, Thrower (1969) on microscopic defects, and Kelly (1969) on thermal conductivity. Thus, the work prior to about 1965 has been adequately summarized, and some specific irradiation damage phenomena are discussed in considerable detail in the above cited literature.

in the 1950s and 1960s were: (1) the Experimental Gas-Cooled Reactor (EGCR) program at Oak Ridge National Laboratory (ORNL), (2) the Dragon Reactor Project [Organization for Economic Cooperation and Development (OECD)] at Winfrith, Dorset, England, (3) the High-Temperature Gas-Cooled Reactor (HTGR) program at Gulf General Atomic Company, and (4) the Kraftverk Pebble Bed Reactor (AVR) program at Jülich, West Germany. In the 1960s the Molten Salt Reactor Experiment (MSRE) was developed. The MSRE design requires that the graphite, which serves as both moderator and structural member, not be penetrated by the fuel salt and gaseous fission products. The graphite must operate at temperatures of 500° to 850°C, but to extremely high fast-neutron fluences in excess of 2×10^{22} n/cm^2.

From this brief account it is obvious that artificial graphite has played a leading role as a high-temperature reactor material. It is currently being utilized or considered as neutron moderator, reflector, structural member, fuel matrix, or control-rod matrix in a number of power reactor projects. The unique properties that make artificial graphite attractive for these functions are its excellent moderating capability, adequate strength at temperatures up to and above 2000°C, good thermal properties, excellent machinability, and relatively low cost. Its low resistance to oxidation has been circumvented by the use of extremely pure helium as coolant, and oxidation is only considered to be a problem in the event of an accident where air or steam can leak into the core.

Graphite, however, shares the common problem that all reactor materials have; that is, it undergoes dimensional and property changes due to damage

It is the purpose of this paper to collect and summarize irradiation data generated during the period 1965 through 1971. This has been a particularly fruitful period, due to the concentrated efforts of a number of investigators to obtain and explain irradiation data at temperatures of 900° to 1400°C to fluences of 2 to 4 x 10^{22} n/cm^2. Considerable effort has been expended in an attempt to understand, at least qualitatively, the basic phenomena of radiation damage by the examination of a variety of materials including near-perfect graphite crystals, both highly oriented and isotropic pyrolytic carbons, conventional anisotropic reactor graphites, and high-strength high-density isotropic graphites. This work has been performed by a number of organizations, which are directly involved in reactor development or support major reactor programs that utilize graphite. Many of the irradiation programs, because of their high cost and complexity, are shared by a number of organizations and their national governments and are indirectly supported by commercial enterprises, notably the major carbon companies in Europe and the United States, by a generous supply of experimental and commercial samples, in-house development programs, and consulting advice.

2. MANUFACTURE

2.1 Conventional Fabrication

The majority of nuclear graphites are produced by the classical Atcheson process employed for half a century in the production of furnace electrodes. This basic technology has been well described in the literature (Nightingale, 1962): a calcined coke filler and thermoplastic hydrocarbon binder are mixed, molded or extruded to form a binder-filler artifact, and subjected to a complex heat treatment to a final temperature of 2600°C or higher. For economic reasons, the heat treatment is generally divided into two stages, baking in gas-heated furnaces to temperatures in the neighborhood of 1000°C followed by "graphitization" in electric resistance-heated furnaces to the final temperature. Because of the porosity introduced by the nature of the raw materials and processing, a liquid impregnant (normally a pitch or tar) is employed prior to or following the first graphitization. The impregnation not only increases the density, but also improves the conductivity, mechanical properties, and uniformity of the finished graphite. Fillers range from ground natural flake to reground artificial graphite and from coal tar pitch cokes through petroleum cokes to Gilsocoke* and carbon blacks. At one time or another, each of these has been considered or used for producing nuclear graphite.

---

*Gilsocarbon-based graphite has achieved a prominent place in nuclear technology due primarily to interest in the United Kingdom. It is made from a coke derived from Gilsonite (a naturally occurring bitumin) presently mined in Utah, U.S.A.

The same flexibility applies to binders and impregnants. Thermoplastic tars and pitches derived from coal or petroleum can be replaced by synthetics derived from pure organic compounds, for example, acenaphthalene and truxene. Thermoplastics may be replaced by thermosetting resins, the most common being those of the furan family. Each of these has found its way into the nuclear field.

It is obviously beyond the scope of this review to consider all the raw material variations in graphite fabrication. The important point is that the selection of filler and binder determines the crystallite microstructure and the associated micropore texture. As will be shown, both have profound effects upon the high-temperature irradiation behavior. Table 1 summarizes the essential fabrication variables for the types of materials referred to in the later discussions of irradiation behavior.

2.2 Nonconventional Fabrication

As the usage of graphite has broadened into areas beyond electrodes and electrolysis applications, and beyond batteries and brushes, very specialized markets have engendered very specialized graphites. The most obvious are those associated with the requirements of the electronics, synthetic chemical, and aerospace industries. The basic Atcheson process, for all its flexibility in raw materials, has proven insufficient. A number of alternative approaches have been studied, which for our purpose are simply referred to as "nonconventional." These materials generally share two characteristics: they are produced in small sizes and are relatively expensive.

TABLE 1
SUMMARY OF CARBONS AND GRAPHITES

Material Types	Raw Material	Manufacturing Details	Structural and Property Description	Irradiation Behavior	Degree of Development and Utility
Single crystals.		Formed in nature.	Represents basic crystal for all polycrystalline artificial graphites. Highly anisotropic in physical and mechanical properties. Relatively free of defects in lattice.	Anisotropic. Relatively stable above 500°C.	Experimental material. Difficult to obtain and handle.
Annealed pyrolytic graphite.	Gaseous hydrocarbons.	Deposited at ∿2100°C and annealed at 2900° to 3600°C.	Similar to single crystals but of lower crystalline perfection.	Similar to single crystals but of lower stability at high temperatures.	Experimental material. Used as a substitute for single crystals because of better integrity and availability as large samples.
Low- and high-temperature pyrolytic carbons.	Gaseous hydrocarbons.	Deposited at 1200° to 2200°C.	Structures range from highly anisotropic to isotropic. Relatively small crystallites. Wide range of mechanical and physical properties and density. Usually nonporous.	Wide range of dimensional changes from anisotropic to isotropic. Stability covers wide range.	Highly developed and useful as coatings for nuclear fuel particles in HTGRs. Structural, property, and irradiation behavior extensively studied.

TABLE 1
SUMMARY OF CARBONS AND GRAPHITES (Continued)

Material Types	Raw Material	Manufacturing Details	Structural and Property Description	Irradiation Behavior	Degree of Development and Utility
Anisotropic graphites manufactured with a binder and filler.	Cokes derived from petroleum. Binder and impregnants usually coal-tar pitch. Cokes calcined prior to manufacture.	Manufactured by conventional techniques. Binder and filler mixed, bodies formed, binder carbonized, bodies heated to 2600° to 2800°C to graphitize structure. Carbon structure results from binder, filler, and impregnant coke.	Characterized by anisotropy in properties. Low thermal expansivity and relatively high thermal conductivity. Relatively weak. Usually coarse grained. Microstructure appears multiphased. Large pores and large spectrum of pore sizes. Relatively soft and easily machinable.	Dimensional and property changes anisotropic. Undergoes rapid expansion at high fluences. Relatively unstable.	Highly developed for a number of commercial applications other than for nuclear use. Manufactured and readily available in large diameters. Considerable production experience and property and irradiation data available. Early extensive use in production and power reactors. Relatively inexpensive and economical for reactor use.
Near-isotropic graphites manufactured with a binder and filler.	Gilsocoke. Binders and impregnants usually coal-tar pitch.	Same as anisotropic graphites above.	Characterized by near-isotropy in properties. Intermediate thermal expansivity and thermal conductivity. Intermediate in strength. Both coarse and fine grained. Microstructure appears multiphased. Large pores and spectrum of pore sizes. Relatively hard and difficult to machine.	Dimensional and property changes slightly anisotropic. Relatively stable in comparison with anisotropic materials. Low expansion rate at high fluences.	Highly developed in United Kingdom for nuclear use. Considerable production experience and property and irradiation data available. Readily available in large diameters. Extensive use in power reactors in the United Kingdom. Intermediate in cost for reactor use.
Near-isotropic graphites manufactured by nonconventional and undisclosed processing methods.	Proprietary cokes and uncalcined cokes derived from petroleum products. Proprietary binders. Possibility that binders are omitted.	Proprietary. Believed to involve isostatic pressing or pressure baking. Heat treatment usually to 2600° to 2800°C.	Characterized by near-isotropy in properties. High thermal expansivity and intermediate in thermal conductivity. Relatively strong, fine grained with small pores and uniform pore size. Relatively soft and intermediate in machinability.	Dimensional and property changes isotropic. Shows high degree of stability in comparison with anisotropic materials. Low expansion at high fluences and delayed to high fluences.	Developed as a specialty graphite for nonnuclear uses. Produced in relatively small diameters and considered experimental for nuclear use. High cost.

Despite the cost and size limitations of these nonconventional materials, they have significant potential for the nuclear industry. First, and most important, some have been found to be more resistant to irradiation damage than conventional graphites. Second, they represent a means to further the study of irradiation behavior of graphites. The production techniques in this area are usually proprietary, and therefore our discussion is limited. Among the techniques employed are:

(1) Hot working: In the thermoplastic range (>2400°C), both pyrolytic graphites and binder-filler graphites may be re-formed by shear and plastic flow. The final product may approach single crystal behavior. This technique appears to be of limited application to the nuclear industry because the extreme anisotropy of the materials is usually undesirable for nuclear applications.

(2) Pressure-baking: The application of pressure during pyrolysis has two effects: it inhibits the evaporation of carbon-containing gaseous pyrolysis products and it promotes crystal growth. Both appear desirable from a nuclear applications viewpoint.

(3) Isostatic molding: This technique combines the advantages of pressure-baking with an external force.

(4) Catalysis: Low-temperature chemical catalysis can be directed at the binder behavior. High-temperature physical catalysis can produce recrystallization. Only the former appears to be important in nuclear applications.

(5) Raw and semicalcined cokes: These filler materials are chemically reactive and produce a "monolithic" graphite structure. In these materials, there are no apparent textural differences from point-to-point in the material at the grain-size level.

The types of nonconventional graphites that are referred to in later sections are also identified in Table 1.

2.3 A Note on Orientation and Fluence

Various terms have been employed to denote orientation, in many cases confusing in that the preferred c-axis direction is perpendicular to the axis of extrusion but parallel to the axis of molding. Both fabrication techniques, however, give rise to cylindrical symmetry. In the following discussions, the notations axial (A), radial (R), or tangential (Tan) are employed with reference to the symmetry axis. To emphasize again, this has no relation to the preferred c-axis orientation until the forming technique is defined.

The graphite irradiation data have been obtained in different test reactors with different neutron spectra. Fluence calculations were made based on different dosimeters and the fluence data have been reported with different neutron energy cutoffs. This makes comparisons of dimensional and property changes difficult.

In an effort to assemble the data, E > 0.050 MeV has been chosen for the purpose of comparison and interpretation of data in this paper. Data in the literature were converted to this scale by the method of Perry and Jenkins (1967).

Perry and Jenkins choice of 0.050 MeV as a lower cutoff for the flux is derived from a damage function analysis for graphite based on neutron energy spectra spanning the extremes available in various reactors. The cutoff is insensitive to the particular model used for the secondary displacement function. At the 0.050-MeV cutoff, the calculated damage rates vary only by 3% at the extremes of the spectral types, which may be contrasted to 23% at the 0.18-MeV limit. Thus, the 0.050-MeV lower limit requires no fluence correction from reactor to reactor and permits direct comparison of all data.

The following table of conversion factors is presented for convenience. A portion of the table was taken from the Dragon and Petten work (Blackstone et al., 1969). The reader is reminded that the conversion of data to E > 0.050 MeV is by calculation for ease of comparison.

TABLE 2
GRAPHITE DAMAGE CORRELATION FACTORS

Facility	Neutron Exposure Expressed as	To Obtain n/cm^2 E > 0.050 MeV Multiply by
Any	n/cm^2 (E > 0.050 MeV)	1.0
High Flux Reactor (HFR)	Equivalent fission fluence	2.0
DIDO, PLUTO	Equivalent Fission Fluence	2.0
General Electric Test Reactor (GETR)/ Engineering Test Reactor (ETR)	n/cm^2 (E > 0.18 MeV)	1.20
Dounreay Fast Reactor	Total dose	0.92

3. IRRADIATION DAMAGE

The graphite lattice is fundamentally damaged in a reactor environment by collision of high-energy neutrons with carbon atoms in the lattice. The carbon atoms are displaced to interstitial positions, leaving behind vacant sites in the layer planes. The interstitial carbon atoms and lattice vacancies either recombine immediately, remain as point defects, or collect into lines or clusters depending upon the conditions of neutron fluence and irradiation temperature and the nature of the graphite structure. The damage to a graphite crystal by high-energy neutrons has been studied directly by transmission electron microscopy where clusters of interstitials and vacancies have been observed in thin sections usually taken from large, well developed crystals.

The early work concerning irradiation damage in graphite has been summarized in a number of articles and books. Thrower (1969) has written an excellent review concerning the use and techniques of electron transmission microscopy as applied to graphite crystals. In his review, Thrower deals with defect structures, material variations, defects produced by elements other than carbon (such as boron), irradiation-induced defects, and nucleation of defect clusters. Reynolds (1968) and Simmons (1962) have also given coherent and precise accounts of the irradiation damage to various types of carbonaceous materials. Earlier de Halas (1962) reviewed the fundamentals of irradiation theory and its application to graphite. Reynolds (1966) also covers

the damage function, point defects, nucleation processes, and other aspects of irradiation behavior in detail. No effort is made here to describe the irradiation damage phenomena in detail; the reader is directed to the above reviews for such detail. The reader is also directed to Thrower (1969) for a complete bibliography of the work prior to 1969 on this subject.

As mentioned previously; high-energy neutrons collide with carbon atoms in the graphite lattice and produce single interstitials and vacancies. Some portion of the vacancies and interstitials are immediately annihilated by recombination, but those remaining may move to nucleation sites and form larger clusters. The magnitude of the clusters is dependent upon the irradiation temperature and fluence. The vacancies remaining in the graphite lattice are immobile at low temperatures and remain as point defects. Above 300° to 500°C the vacancies become mobile, and it is speculated that the vacancies can be formed into lines. These lines collapse when they grow to a critical length and then continue to grow by capture of more vacancies at the ends (Kelly, 1969), resulting in shrinkage of the crystals in the a-axis direction. Interstitial clusters cause crystal growth in the c-axis direction. This general description of irradiation damage in the graphite lattice is deduced from transmission electron microscopy observations in large single crystals or highly annealed pyrolytic carbons, which approach the natural crystals in perfection. As the irradiation temperature is increased from 150° to 1350°C, the interstitial loops or clusters increase in size and decrease in density (Thrower, October 1968a). These reactions have been explained in terms of a theory of homogeneous nucleation assuming that the loops are nucleated by the chance encounter of two slowly moving groups of

atoms and that they grow by the addition of single interstitials. The diffusion was assumed to be two dimensional and to occur solely within the basal plane.

Recently Turnbull and Stagg (1969) have introduced the concept of three-dimensional diffusion to explain the kinetics of annealing large interstitial and vacancy loops. Turnbull and Stagg observed c-axis diffusion above 2000°C in thermal annealing experiments on single crystals. Thrower (October 1968a) reasoned that in polycrystalline reactor graphites, which have smaller crystallites, there may be c-axis diffusion as low as 1000°C in a neutron flux and migrating defects may find sinks between basal planes rather than at crystallite edge sites. Thrower (October 1968b) has been a major contributor to the irradiation damage field in the past 5 to 6 years and has developed a number of ideas concerning defect nucleation based on his observations of highly perfected crystals and reactor graphites. He examined pyrolytic graphites whose crystallite perfection in the basal plane was excellent, comparing favorably with that of single crystals, but whose perfection in the c-direction could be varied over a wide range. Two materials were studied: (1) pyrolytic graphite heated to 2900°C, and (2) a second pyrolytic graphite stress-annealed at 3300° to 3600°C. These were the same carbons as those used by Kelly for dimensional change measurements. Kelly (1966) describes these carbons in detail. They were irradiated at 1350°C along with single crystals to $\sim 2.34 \times 10^{21}$ n/cm^2.

At 1350°C the nucleation of irradiation damage in thin crystals of the 2900°C material did not proceed as in single crystals. Vacancies were

homogeneously nucleated throughout the crystal, as there were no larger interstitial loops to introduce the heterogeneous nucleation previously observed in single-crystal studies. Since the crystallite perfection in the basal planes was equal to that of single crystals, Thrower concluded that the other crystallite dimension must be responsible for the apparent loss of interstitials and the majority of interstitial atoms had migrated to twist boundaries where they formed very large loops. The observation of these faint loops was always found to be associated with the presence of twist boundaries. Thrower concluded that the large population of interstitial atoms in the form of an irregular loop within twist boundaries migrated along the c-axis by interstitial diffusion during irradiation at 1350°C.

Thrower believes that in single crystals the interstitial loops grow from nuclei by the addition of the faster moving interstitial atoms. Any motion of a loop is confined within its plane and interstitial loops or clusters are not expected to occur in twist boundaries. He assumed the large interstitial loops in the twist boundaries were formed by the diffusion of single interstitials in the c-axis direction.

Interstitial diffusion along the c-axis is expected to occur at temperatures of 900°C and above and becomes significant before vacancy migrations take place within the basal plane. The interstitial loops in single crystals were found to be much smaller than those in the 2900°C material were many twist boundaries are present.

Thrower admits this work does little to clear the confusion about the nucleation of defect groups in high-temperature reactor graphite. When damage is observed, it is usually in an exceptionally large crystallite which may not be characteristic of the material as a whole.

In a later paper Thrower (July 1971) carried his studies on the same materials to higher fluences and observed, at higher neutron fluences, that as the number of vacancies in lines increased, the number of surplus interstitials also increased. He again emphasized the difficulties of observing defects in such highly damaged crystals, and it was impossible to estimate size, shape, or density of the nucleated defects.

Thrower (May 1971) irradiated reactor graphites at 1300°C and attempted to identify the irradiation defects. From observations in the highly crystalline particles, he found defects trapped at twist boundaries. Thrower believes that the density of nonbasal dislocations in reactor graphites is an order of magnitude higher than those in well oriented pyrolytic graphite and therefore the c-axis diffusion may occur at temperatures lower than 600°C in this type of graphite. He expects the nucleation of interstitial atoms in highly crystalline particles of reactor graphites to have three temperature regimes where (1) nucleation is homogeneous and uniform throughout the crystallites ($T \leq 300°C$), (2) nucleation occurs at crystallite boundaries and at some boron impurity atoms, the total amount of nucleated damage decreasing with temperature ($350°C \leq T \leq 650°C$), and (3) where an increasing number of interstitials are lost to twist boundaries where they are unannealable ($T \geq 350°C$). This should cause the retained

interstitial damage to increase quite markedly from 650° to 1200°C, as observed by Bokros et al. (1968). For irradiations at 900° and 1200°C, vacancies may nucleate within the highly crystalline material, but at 1200°C the number of clusters observed is quite small and some crystallites contained none at all. In the highly crystalline particles, three temperature regimes were defined where (1) vacancies are immobile and mostly single ($T < 600°C$), (2) nucleation is uniform and homogeneous ($650°C \leq T \leq 1100°C$), and (3) loss of vacancies to crystallite boundaries causes an unannealable contraction in the a-axis ($T \geq 1100°C$). He expects this model for highly crystalline particles to apply to the less perfect crystallites at lower temperatures for each effect. However, this has not been confirmed since nucleated defects have not been observed in the less crystalline particles of reactor graphites for irradiations above 900°C (Thrower, May 1971). On the basis of the model one might expect larger dimensional changes in the less crystalline particles.

Thrower believes the defect configuration providing maximum dimensional stability occurs when both vacancies and interstitials are nucleated into large loops. The most likely situation for this to occur would be at about 900°C in highly crystalline materials, and he expects the bulk volume change of a graphite at this temperature to be related to its fraction of highly crystalline structure.

Hinman et al. (1970) irradiated natural flake graphites and measured vacancy concentrations in specimens irradiated by neutrons or by carbon ions up to fluences corresponding to 10^{-5} to 10^{-4} displacements per lattice

site. They found an increase in vacancy concentration with increasing temperature, which is contrary to expectation because higher temperatures should lead to a smaller cluster density, a condition which favors interstitial-vacancy recombination.

Hinman does not believe that interstitial-vacancy recombination increases with fluence, since the number of interstitial clusters increases. He speculates that collapsed vacancy line clusters, probably largely divacancies which have become sufficiently numerous in the fluence range of his studies, absorb a large number of vacancies. An increasing number of these sinks will produce a decreasing vacancy concentration; this effect should show up at high fluences.

If Hinman's explanation is correct, it suggests that the vacancies are more mobile than is generally assumed, or, alternatively, that a collapsed divacancy is mobile. It appears, therefore, that the small interstitial clusters which are formed as a result of neutron irradiation may be stable over a wide range of irradiation and annealing temperatures.

Heerschap and Schüller (1969) have published electron micrographs from samples irradiated at 900° and 1200°C. They found interstitial loops upon irradiation at 900°C with small defects in the center of the loops that resembled vacancy clusters. The interstitial loops grew upon irradiation at 1200°C, while the small vacancy loops grew at the periphery of the interstitial loops.

Reactor graphites still defy direct examination due to difficulties in specimen preparation and problems in interpreting the complex defraction patterns. However, some observations have been made in the crystallites of highest order in reactor graphites and the pyrolytic data have been interpreted to show that c-axis diffusion may occur at lower temperatures in the smaller, less perfect crystallites of reactor graphites. However, there appears to be little doubt that an increase in crystalline perfection of the graphite structure will improve the irradiation stability of the crystallites, and at high temperatures the damage retained in a reactor graphite will be related to its fraction of highly crystalline structure.

4. DIMENSIONAL AND STRUCTURAL CHANGES

4.1 Introduction

Dimensional changes in the graphite moderator are important to the reactor designer. The dimensional behavior of the graphite must be known as a function of the reactor operating temperature, temperature history, and the expected fast fluences of the particular reactor under consideration. Two criteria usually determine the usefulness of the graphite in reactor design: (1) the maximum contraction, which influences the stability of a graphite stack, and (2) the fluence where net dimensional expansion commences at high fluences. Therefore, it is very important to irradiate graphites at temperatures and fluences that include and extend beyond the design conditions of current graphite-moderated reactors.

Helm (1964) and Perks and Simmons (1966) have shown in early work the general characteristics of reactor graphites under high-energy neutron irradiations at temperatures from 300° to 800°C to fluences of 2×10^{22} n/cm^2, e.g., initial contraction followed by expansion. More recently (1965 through 1971) a wide variety of experimental and commercial reactor graphites (see Table 1) have been irradiated at higher temperatures and fluences by a number of investigators from the Dragon Project, Petten, and KFA (Jülich) in Europe and from Battelle Northwest Laboratory, Oak Ridge National Laboratory,

and Gulf General Atomic Company in the United States. These irradiation experiments included temperatures of up to 1400°C and fluences of 4×10^{22} n/cm^2.

4.2 Single Crystals and Highly Oriented Graphites

Before attempting to discuss bulk dimensional changes in reactor graphites, it will be helpful to first review the irradiation behavior of near-single crystals, annealed pyrolytic carbons, and highly oriented graphites. These materials are essentially nonporous and have highly aligned crystallites in comparison with the artificial reactor graphites; measurements of their bulk dimensional changes more nearly approximate their crystallite changes.

It is noteworthy to mention that due to the differences in microstructure, orientation, and porosity between the highly aligned carbons and the complex reactor graphites, only qualitative deductions are possible in explaining the behavior of the reactor graphites. However, a considerable amount of information concerning fundamental changes in the graphite structure and crystallite dimensional change rates may be obtained from these materials, and the value of irradiating such materials for the purpose of learning more about the behavior of reactor graphites is immediately obvious.

A number of investigators have studied single crystals, highly annealed pyrolytic carbons, and pyrolytic carbons deposited at relatively low temperatures (Price, 1969; Kelly and Brocklehurst, 1971; Bokros et al., 1968; Bokros

and Price, 1967; Bokros and Koyama, 1970). Dimensions of highly aligned materials changed linearly with fluence and the dimensional change rate decreased with increasing apparent crystallite size (Price, 1969; Kelly and Brocklehurst, 1971; Bokros et al., 1968). The data of Price (1969) at 1225° to 1300°C are shown in Figure 1 to illustrate this point. The dimensional change rate for materials with L_c values of 220 Å is about a factor of 10 higher than for materials with L_c values of 750 to 1600 Å. However, highly crystalline pyrolytic samples containing 0.5% boron were found to change dimensions at the same rate as poorly crystalline as-deposited undoped samples, indicating that boron can nucleate additional damage centers in crystalline material (Kelly and Brocklehurst, 1971). A group of boron-doped samples annealed at temperatures between 2200° and 3000°C and irradiated at 930°C to 2.0×10^{21} n/cm^2 showed dimensional change rates decreasing with increasing annealing temperature in a manner very similar to those shown by Price's data in Figure 1. The dimensional change rates were found to be inversely proportional to the crystallite width, L_a, deduced from thermal conductivity measurements.

4.3 Pyrolytic Carbons

Due to the high level of interest in pyrolytic carbon coated fuels for HTGRs, there has been a parallel effort to that for the graphites to determine the dimensional and structural changes in pyrolytic carbons over the same temperature and fluence ranges as for the graphites. These data are of value in the interpretation of reactor graphites.

In pyrolytic carbons where crystallite size and density are the same, isotropic bodies were found to be the most stable (Bokros and Price, 1967; Bokros and Koyama, 1970; Kaae, Stevens, and Bokros, 1971). If other factors are held constant, increasing the degree of crystalline perfection increases the dimensional stability of the carbons especially at irradiation temperatures above 800°C. At high fluences, and especially at temperatures >1000°C, crystallite interactions may become more important than crystallite size; a qualitative interpretation of these effects has been given by Engle and Bokros (1971).

It was observed during irradiation at low fluences that high-density nominally isotropic carbons shrink isotropically. At higher fluences, especially at high irradiation temperatures, these materials start to behave anisotropically, shrinking in the direction parallel to the deposition plane and expanding in the perpendicular direction. As a result, at low fluences high density enhances stability, but at high fluences high density leads to instability (Kaae, Stevens, and Bokros, 1971; Engle and Bokros, 1971).

Carbons that have small crystallite sizes have high strength, and it is believed that such a structure is important to minimize pore generation at high fluences. This observation that materials with small crystallites will be more stable than those with large crystallites appears to contradict the data from Section 4.2, but it will be shown that strength and isotropy may be important in inhibiting structural degradation in the carbons and reactor graphites. This does not mean that the crystallite size effect is not valid, but rather that microstructural effects can dominate in polycrystalline materials.

Bokros (Engle and Bokros, 1971; Kaae, Bokros, and Stevens, 1971) suggests that at some intermediate irradiation temperature, $T_{(max.\ int.)}$ (see Figure 2), effects such as exaggerated volume expansion, rapid degradation of crystal structure, and accelerations in the dimensional change rate will be a maximum. The interactions will be most pronounced for the isotropic carbons of highest density. At high temperatures and especially near $T_{(max.\ int.)}$, high density will contribute to dimensional instability. At high fluences the stronger but less crystalline low-density carbons do not expand as much and do not exhibit the large accelerating effects observed for high-density carbons (Bokros and Stevens, 1971; Bokros et al., 1971). Bokros further suggests that the effects of mechanical interactions between crystallites are less effective in causing pore generation and accelerations in dimensional change rates for materials with extensive crosslinking and strong internal binding. With the possibility of higher internal stresses in the stronger carbons, the crystallite strains are more likely to be accommodated by irradiation-induced creep. Thus, increasing the strength by decreasing the crystallite size may result in a net improvement in the dimensional stability of the polycrystalline carbon in spite of the lower stability expected for smaller crystallites in the unrestrained condition.

4.4 Reactor Graphites

We can now turn our attention to the discussion of reactor graphites. Here the situation is far more complex and difficult to analyze. The complexity in reactor graphites is due to the derivation of raw materials from nonhomogeneous carbonaceous precursors of the filler cokes and binders, the

multiphase granular-type formulation methods, and complex processing as described in Section 2.

Although the microstructure of reactor graphites is of such complexity, their high-temperature behavior, as will be shown at least qualitatively, is quite similar to that of the pyrolytic carbons.

High-temperature high-fluence dimensional change data representative of conventional anisotropic petroleum-coke graphites have been selected from the work at Battelle Northwest Laboratory (BNWL), Gulf General Atomic Company, the Dragon Project, and Oak Ridge National Laboratory (ORNL) (Cox and Helm, 1969; Eatherly and Kennedy, 1971; Engle and Bokros, 1971; Gray and Pitner, 1971; Hankart et al., September 1971). These data are presented in Figures 3 and 4. The dimensional curves are all similar in shape and are in agreement with the earlier data (Helm, 1963; Perks and Simmons, 1966). The graphites shrink initially in the preferred c-axis direction and turn around and expand at higher fluences. In the a-axis direction the contraction rate is initially higher, and the saturation or turnaround to expansion occurs at higher fluences and has not been reached in all cases. The anisotropic behavior is caused by the high degree of alignment of the crystallites within the anisotropic filler particles and the subsequent high degree of alignment imparted to the filler particles by the forming methods. There is a marked effect of irradiation temperature in the range 700° to 1300°C on the magnitude of the dimensional changes for a particular grade of graphite, as illustrated by the data of Gray and Pitner (1971) of BNWL. The Battelle data show only a small difference in behavior in the range 400° to 750°C: early turnaround

followed by rapid expansion at 950° to 1050°C and slower expansion rates again above about 1200°C.

The data in Figure 5 taken from the Dragon Project, BNWL, and Gulf General Atomic Company illustrate the dimensional behavior of graphites manufactured with Gilsocoke (Blackstone et al., 1969; Blacksone et al., 1971; Engle and Bokros, 1971; Engle and Pitner, 1970; Hankart, et al., June 1971). The Gilsocarbon materials, while considerably more isotropic than the petroleum coke materials, still exhibit some anisotropy in their dimensional changes. The dimensional changes of these materials, in comparison with the anisotropic petroleum-coke graphites, show less total contraction, lower expansion rates after turnaround, and a delay in turnaround until higher fluences.

Data from BNWL and ORNL on high-density isotropic materials are presented in Figures 4 and 6 (Eatherly and Kennedy, 1971; Pitner, 1971). These materials are essentially isotropic in irradiation behavior and are considerably more stable in their dimensional changes than the conventional binder-filler materials. At 500° to 750°C measurable dimensional changes do not occur until 7×10^{21} n/cm^2. At 1000° to 1100°C expansion begins immediately, but the rate of expansion slows at relatively low fluences. At 1200° to 1300°C, these materials begin to contract in a manner similar to the binder-filler materials, but the magnitude of the contraction is small, expansion is delayed to high fluences, and the expansion rate is low.

Photomicrographs illustrating the microstructures of these three classes of graphite before irradiation and after expansion at high fluences are shown in Figure 7.

Another class of graphite based on carbon black fillers has received renewed attention recently at ORNL (Eatherly and Kennedy, 1971) (see Figure 4). Above about 7×10^{21} n/cm^2 these materials exhibit an isotropic linear expansion at 750°C. Unfortunately high-fluence data at higher temperatures are not available.

It is noteworthy that in the range 900° to 1200°C, the breakaway expansion appears to accelerate with increasing temperature, but above 1200°C it appears to slow again. There is considerable uncertainty on this point, and the data from various investigators (see Figures 3 and 5) appear to conflict somewhat in the transition range from 1100° to 1300°C. Additional data are needed to further clarify the behavior of reactor graphites in the range 900° to 1400°C.

Detailed structural examinations of reactor graphites before and after irradiation to high temperatures and high fluences have been made by Thrower (May 1971) using X-ray diffraction and replica and transmission electron microscopy and by Engle using a densimetric separation technique coupled with X-ray diffraction and scanning electron microscopy (Engle, 1970; Engle, August 1971; Engle and Bokros, 1971).

Thrower (May 1971) examined eight graphites, for which dimensional change data had been obtained at 900° to 1300°C, for structure and composition. Using electron transmission microscopy at magnifications of about 25,000, Thrower attempted to identify different components of the graphite structures. He identified four distinctly different types of particles, not

all necessarily in any one graphite: (1) highly crystalline particles, (2) a highly crystalline-appearing particle, but also highly deformed, (3) needle-like or whisker-type particles (found in Gilsocarbon graphite), and (4) a circular particle composed of needle or lamilar crystallites arranged in concentric circles as rosettes. Thrower concluded that only PGA, a highly oriented graphite, contained highly crystalline particles, whereas the other materials, which were isotropic, were multiphased.

In his discussions Thrower considers the mean basal-plane separation of boundaries which scatter phonons (L_p) rather than the X-ray determined (L_a) distances to describe the crystallite size. L_p is about 3 to 5 times larger than L_a and contains a number of low angle tilt boundaries which do not scatter phonons. Thrower believes basal plane diffusion of interstitials can proceed through the low angle boundaries within L_p, but not the boundaries which define L_p, and therefore L_p is a better measure of crystallite size in the a-axis direction. He concluded from experiments in pyrolytic carbons (Thrower, October 1968a) (discussed in Section 3) that interstitial defects may escape to basal plane twist boundaries by c-axis diffusion and nucleate in the twist boundaries. He then assumed that a high-temperature defect will behave similarly in artificial graphites and in pyrolytic materials since both have similar L_c values.

Thrower examined the graphites by transmission electron microscopy after irradiation to fluences of up to 6×10^{21} n/cm^2 at 900° or 1300°C. He observed defect clusters only in the highly crystalline particles. However, he admits "poor diffraction conditions in the reactor graphites made an

unambiguous identification of these defects impossible." He reasoned that even though L_p values are 5 times greater in the annealed pyrolytic graphite than in reactor graphite, this should not be important since the scale of interstitial nucleation is greater than the crystallite size in either material whether one uses L_a or L_p.

He found no effect on the deformed particles, although he believes similar defects to those in the highly crystalline particles could possibly exist, but may be hidden by the varying contrast conditions. In crystallites of the needle form there was some effect, but no nucleated defects were observed and a simple breakdown of the structure was observed. The initial mass of needle-type particles resembled a sponge after irradiation. There were also signs of structural degradation in the less crystalline or rosette particles.

At very high temperatures (>1200°C), Thrower expects the dimensions of the highly crystalline particles to change, but to maintain a constant crystallite volume since the vacancies and interstitials are separated by the latter diffusing along nonbasal dislocations. The needle-like crystallites give better dimensional stability than the rosette arrangements after irradiation at 900°C.

Engle (1970) also examined a number of graphites by a technique of comminuting the graphites to small particles (0.1 to 40 μm) followed by separation according to their liquid immersion density. The density fractions were examined for structure by X-ray diffraction and scanning electron

microscopy. Engle found that anisotropic needle-coke reactor graphites, especially those that had been impregnated, contained a wide range of crystallite sizes (L_c values from 350 to 1600 Å) varying systematically with particle density, whereas near-isotropic materials such as Gilsocarbon graphites had a narrow band of crystallite sizes (350 to 550 Å). High-density isotropic graphites which have no observable binder phase were found to have crystallite sizes of about 400 Å with little variation. Micrographic and scanning electron microscopy studies showed the particles from low-density fractions of the needle-coke graphites to be equiaxed and isotropic, whereas those from the high-density fractions were needle-shaped and anisotropic.

Porosity was identified in three domains of the graphite microstructures: intercrystallite pores or defects, pores that are external to the individual density-fraction particles but closed to measuring liquids in the bulk sample, and large open pores due to grist particle mismatches or frozen in pores that formed during carbonization and graphitization. This technique allows a qualitative evaluation of structural changes during irradiation (Engle, August 1971; Engle and Bokros, 1971). The results are illustrated by the series of density curves in Figure 8. The bulk volume contraction rates were found to be similar for a weak, anisotropic graphite and a strong, isotropic graphite (see Figure 8a), but the bulk volume expansion rate after turnaround was much higher for the weak, anisotropic material (also compare data in Figures 3, 4, 5, and 6). This behavior was also found for the solid structure (see Figure 8b). However, crystallite clusters (defined as the small sink-float particles) (Engle, 1970) of both types of

material expanded immediately during initial bulk contraction, with the weaker, highly oriented graphites expanding at a greater rate than the stronger isotropic graphites (Figure 8c). Pores extending over dimensions much larger than crystallite dimensions and located between crystallite clusters were found to be eliminated during densification, apparently by the crystallite c-axis expansion. The rate of elimination of these pores increased with increasing irradiation temperature.

The surprising aspect of this experiment was the observation that the mean value of the crystallite clusters (represented by the mean density of the sink-float particles) was observed to decrease in all graphites, while the solid and bulk densities were increasing (see Figure 8). This suggests that microporosity is generated immediately at the crystallite level causing expansion of the crystallite clusters, and that accommodation of c-axis expansion results from closure of much larger cracks or pores which extend through the microstructure over much larger distances than crystallite dimensions rather than pores associated with crystallites.

Pores were observed to form between filler particles during the expansion phase at high fluences, accounting for the large volume expansions of the graphites (see Figure 7). The ease of formation of these pores and cracks and the expansion rate after turnaround were found to be, in a qualitative manner, dependent on the volume percent of highly graphitic (low-strength) material in the structure. These results were consistent with those obtained concurrently on the pyrolytic carbons, i.e., that strong isotropic structures are more stable than anisotropic structures during high-temperature irradiation.

The complex behavior of artificial bodies at high fluences was interpreted qualitatively by Engle and Bokros based on their studies of pyrolytic carbons and reactor graphites (Engle and Bokros, 1971). As the crystallites in an aggregate change shape, the interactions between crystallites are at first accommodated by internal porosity. Under these circumstances, the behavior of the bulk is controlled by the behavior of unrestrained crystallites. At high fluences, however, when the internal porosity is nearly gone, the interactions between crystallites become intense. Stresses between crystallites rise and new pores form either by stress-directed diffusion of vacancies or by fracture at boundaries. As a result of these interactions, the crystal structure is degraded, causing an acceleration in the rate at which the crystallites change dimension and in pore generation. Pore generation is retarded in the high-strength, isotropic graphites and the explanations given previously for pyrolytic carbons hold for the graphites.

Pitner (July 1971) and Gray and Pitner (1971) irradiated about 20 grades of graphite to 15 x 10^{21} n/cm^2 at 1000° to 1200°C. At 1000° to 1200°C they found that dimensional distortions were similar to those observed at lower temperatures but that they occurred at a higher rate. Above 1200°C the expansion rate after turnaround in the radial direction was considerably reduced from that at 1000° to 1200°C (see Figure 3). Dimensional changes of high-density, high-strength isotropic graphites with high thermal expansivity values ($\sim$7 x 10^{-6} $°C^{-1}$) were more isotropic and of lower magnitude than those of anisotropic materials, turnaround was slower, and expansion was delayed. The isotropic graphites showed rapid expansion at the onset of irradiation but decreased to nearly zero for high-density materials and became negative

for low-density materials after 2×10^{21} n/cm^2. Expansion again became prevalent after 10^{22} n/cm^2, but the rate of expansion was less than for anisotropic graphites. Above 1200°C these graphites contracted slightly.

Gray and Pitner believe the slower expansion rates observed above 1200°C, in comparison with those at 1000° to 1200°C in their experiments, can be explained by invoking a higher creep constant that allows plastic deformation rather than fracture to accommodate differential crystal strains (Gray and Pitner, 1971).

Pitner (October 1971) (see Figure 6) has irradiated fine-grained, isotropic, high-strength, high-CTE materials. These materials represent a growing class of graphites that have a very uniform structure with small, equiaxed filler particles that are difficult to distinguish (see Table 1). No continuous binder phase is evident in this class of graphites, and the binder-filler separation that is present along the basal plane surfaces of the filler particles in the needle-coke graphites is not seen in these materials. Intraparticle cracks are also absent.

Pitner found these materials to expand with fluence (see Figure 6) during the early stages of irradiation at ∿1000°C, and quickly saturate at low fluences whereas conventional graphites contracted. Pitner believes that under irradiation, the c-axis expansion of the crystallites in the binderless materials appears immediately as a bulk expansion at low fluences rather than being accommodated by basal plane cracks, which is believed to occur in conventional anisotropic graphites.

At ∿1000°C and after high neutron exposures (>10^{22} n/cm^2), these graphites began to expand again, apparently corresponding to the ultimate high-exposure expansion seen in conventional graphites. However, this growth took place at a significantly delayed fluence and reduced rate from that of conventional graphites. Pitner postulated that this improved behavior may be due to the exceptionally good bonding quality among the particles, as evidenced from their high strengths. Distortions generated by particle expansions may be restrained by tight bonding among the particles, allowing irradiation creep to accommodate some of the strains without fracture. Consequently, the large degree of crack generation associated with high-exposure expansion in conventional graphites may not be observed in these materials, and the growth rate may be reduced. The structural integrity at high fluences was substantiated by strength measurements.

At temperatures above 1200°C, these materials contracted from the onset of irradiation rather than expanding. This behavior was believed to be due to the increased irradiation-induced creep rate of the graphite at temperatures above 1200°C.

Low-density grades of high-strength isotropic graphites (ρ = 1.5 g/cm^3) were also irradiated and appear to have increased lifetimes over the higher density grades (ρ = 1.8 g/cm^3). This is believed to be true because at 950° to 1100°C, the initial expansion for the low-density materials was followed by contraction to a point less than the original sample length, and the ultimate high-fluence expansion was also delayed. Above 1200°C the greater contractions also suggest that higher exposures will be reached before a net expansion is experienced.

Blackstone et al. (1969, 1971) irradiated Gilsocarbon graphites at 900° and 1200°C (see Figure 5). In these studies they attempted to correlate on a statistical basis relationships between properties such as Young's modulus and density and irradiation behavior. They could not establish correlations between preirradiation properties and dimensional changes except that a high initial Young's modulus was associated with a higher initial contraction rate at 1200°C.

In connection with the molten-salt reactor program, Eatherly and Kennedy (1971) have investigated the behavior of graphites at 700°C to fluences up to 4.5×10^{22} n/cm^2 (see Figure 4). This program is noteworthy for the wide variety of materials investigated, many of which were fabricated at ORNL or at the Y-12 Development Laboratory (Kennedy, 1970; Overholser, 1969). Hence the raw materials and fabrication history are completely known. Included in this work are sets of materials with approximately the same crystallite size but varying orientation paramters. Since the volumetric changes taking place in the bulk material involve both the crystallites and pores, it is generally not possible to deduce the crystallite behavior from the bulk behavior. Kennedy (1969, 1970) has hypothesized that the changes in pore volume would not be significant when the rate of change of bulk volume with fluence is zero, an assumption that would be exact if the pores were not preferentially oriented and the crystallites were changing shape at constant volume. Thus, the linear dimensional changes occurring at the instant the volume change rate goes to zero are characteristic of the crystallite dimensional change rates. He thus obtains curves similar to those of Bokros and Price (1971) for

pyrolytic carbons, and the crystallite growth rates in bulk artificial graphite are identical to those obtained by Bokros and Price (1967).

These investigators have also divided their material into three general classes, based upon their dimensional behavior (Eatherly and Kennedy, 1971). The first class is defined as conventional in the sense of Section 2, and is characterized by rapid shrinkage followed by rapid expansion along a roughly parabolic curve. The second class is termed monolithic (high density, high strength), and is characterized by a long induction period of relative stability before parabolic expansion occurs. The third class is graphites based upon blacks as fillers, which possess a linear expansion curve above 7×10^{21} n/cm^2 at 715°C (see Figure 4). Eatherly (1969) has derived an equation based on unrestrained crystal growth with resultant pore generation which results in a parabolic breakaway expansion and predicts both the magnitude and orientation effects.

They believe the long induction period of the monolithic-type graphites is associated with the pore texture and a high degree of plastic flow. The ORNL group has utilized raw isotropic cokes (such as those made from air-blown asphaltenes) coupled with intensive mixing to produce monolithic graphites. The resultant materials had relatively high expansion coefficients, isolated spherical pores, and high strain-to-failure. The monolithic-type structure, in this case at least, is attributed to the high chemical activity of the raw coke and its interaction with the binder.

Delle (1971) and Delle and Vohler (1971) discussed the influence of the raw materials used for the manufacture of nuclear graphites on their

behavior under high-flux fast-neutron irradiations and studied resulting changes in linear dimensions and physical properties, in particular the influences of different grain types, binder types, and binder contents.

In describing their data, Delle and Vohler assumed that polycrystalline graphite consisted of well and poorly ordered regions, similar to the early ideas of de Halas and Yoshikàwa (1962). Delle presents an equation to represent dimensional changes and indicates it is possible to take account of the irradiation-induced ordering of poorly graphitized regions by a shrinkage term. An expansion term was added allowing for lattice expansions in the c-direction, as well as a shrinkage term allowing for the lattice contraction in the a-direction. The expansion is reduced by porosity; i.e., the crystallites may expand into the pores while the dimensions of the bulk are not affected to the same extent. When the pores close at sufficiently high fluences, the expansion term increases and predominates over the shrinkage term. Such pores are more abundant in graphites based on pitch or petroleum cokes, but are not abundant in natural graphites. The expansion in natural graphite therefore predominates at relatively low fluences.

Delle believes from oxidation studies that the binder coke composes the poorly graphitized regions of the bulk material and that the shrinkage term becomes higher with increasing binder content. A higher shrinkage is obtained by the use of resin binders instead of pitch binders where processing is apparently otherwise the same.

Delle and Vohler discussed the expansion of graphites after turnaround. Beyond the turnaround of the dimensional changes, a relative increase in the porosity was observed as a result of the development of new micropores due to internal stresses during the expansion of the crystallites and the newly developed macropores. The newly formed porosity was quite different from that before irradiation with respect to pore size distribution and the total size of the pores.

The behavior of four extruded graphites was discussed by Nettley and Martin (1966). All four graphites were manufactured from cokes and binders that yielded well graphitized material when they were heat treated at about 2800°C. The materials included an anisotropic graphite (PGA) and three near-isotropic graphites. They found the crystal strains in poorly graphitized material to be much larger than those in the well graphitized material when they were irradiated under similar conditions.

4.5 Models to Explain Dimensional Changes

A number of authors have attempted to relate structural characteristics and properties such as thermal expansivity, crystallite orientation, and crystallite change rates to bulk dimensional changes in artificial graphites and pyrolytic carbons. It is considered worthwhile to review the early work briefly and to present the more recent ideas.

Simmons (1959, 1961) first proposed the following expression based on thermodynamic considerations:

$$\frac{\ell d\ell_x}{\ell_x d\gamma} = A_x \frac{\ell dX_c}{X_c d\gamma} + (1 - A_x)\frac{\ell dX_a}{X_a d\gamma} \quad ,$$

where ℓ_x is the length of the body in a particular direction x, γ is the fast-neutron exposure, X_c is the dimension of an individual crystallite in the c-direction, and X_a is the crystallite dimension in the a-direction. A_x is a parameter characteristic of the direction of measurement, x, in a particular block of graphite. It is related to the way stress applied to the bulk material is distributed in the crystallites.

In practice, A_x is obtained from the thermal expansion coefficient, α_x, of the body in the x-direction, using an expression analogous to the one used for irradiation-induced dimensional change:

$$\alpha_x = A_x \alpha_c + (1 - A_x)\alpha_a \quad ,$$

where α_c and α_a are the single-crystal thermal expansion coefficients at the temperature of measurement. The derivation assumes that the material acts as a single phase. It is assumed that the effects of pores and microcracks are accounted for by their influence on the stress distribution among the crystallites and hence on A_x.

An alternative but similar treatment by Price and Bokros (1965) follows work on the thermal expansion of polycrystalline graphite by Bacon (1956) and by Sutton and Howard (1962). The bulk dimensional change is obtained by averaging the dimensional change of the constituent crystallites, taking

into account the preferred orientation of the body. Part of the c-direction crystallite expansion is accommodated by the cleavage microcracks lying parallel to the basal plane. The resulting expression for the irradiation-induced dimensional change has the form:

$$\frac{\ell d\ell_x}{\ell_x d\gamma} = (1 - R_x)\Gamma_x \frac{\ell dX_c}{X_c d\gamma} + R_x \frac{\ell dX_a}{X_a d\gamma} \quad .$$

R_x is a preferred orientation parameter that may be obtained from X-ray diffraction measurements and depends on the degree of preferred orientation and the direction of measurement within a body.

The "accommodation coefficient," Γ_x, is the fraction of crystallite expansion in the c-direction that contributes to the bulk dimensional change. It is a function of the preferred orientation of the body, of the direction of measurement, and of the details of the microstructure. In practice it is obtained from measurements of the thermal expansion coefficient of the body in the required direction x, and the following formula:

$$\alpha_x = (1 - R_x)\Gamma_x\alpha_c + R_x\alpha_a \quad .$$

The derivation again assumes that the material acts as a single phase. The effect of the basal-plane microcracks is taken into account by the accommodation coefficient Γ_x. The effects of bulk porosity, intercrystallite elastic restraints, and accommodation of the crystal a-direction changes are neglected.

The two models are identical for an idealized case of a crack- and pore-free aggregate without intercrystallite restraints. Both models explain the general features of the observed irradiation-induced dimensional changes in a sample of polycrystalline graphite in terms of a crystallite c-direction expansion and an a-direction contraction. The increases in the thermal expansion coefficient and the irradiation-induced growth rate perpendicular to the extrusion axis that occur at the "breakaway" point during irradiation are explained in both cases by closure of the oriented microcracks.

The validity of the equations was tested by Price and Bokros (1967) by measuring the dimensional changes in an oriented graphite body. Price and Bokros found that the agreement between measurements and the relationships predicted by the single-phase models for irradiation-induced dimensional change in artificial graphites showed such models to be valid for irradiations in the temperature range ∿500° to 1100°C and fluences up to 3×10^{21} n/cm^2, and the Simmons model fitted the data slightly better than the alternate model. The additional shrinkage in any nongraphitic material that may be present was not sufficient to affect the single-phase relationships.

Perks and Simmons (1966) and Henson, Perks, and Simmons (1968) have continued the irradiation of graphites begun in their earlier work to higher temperatures and fluences, where the graphites have turned around and expanded, and have presented some further ideas dealing with the analysis of dimensional changes.

Perks and Simmons (1966) showed their previous relationships (Simmons, 1959, 1961) to break down at high irradiation fluences. At high fluences they speculate that restraints may not be the same for thermal expansion and irradiation growth due to the effect of irradiation creep. These authors suggest how their theory of dimensional changes should be modified to take into account the effects of irradiation creep.

They speculated that the pore space diminishes in the early stages of irradiation and at high fluences there is some pore generation in their anisotropic graphite. They further concluded that the increase of pore volume in their anisotropic graphite at high fluences occurs between the grist particles. The effect does not appear in the isotropic graphite, presumably because the grist particles are more nearly isotropic than those of the anisotropic graphite.

They believe from the theory outlined that a material composed of isotropic particles would, after initial effects due to closure of the cracks and volume expansion of the crystals, become stable at high fluences.

Further work by Henson, Perks, and Simmons (1968) concerned measurements made on graphite irradiated at 900° and 1350°C, at 400° to 450°C, and at 550° to 650°C. Lattice parameter changes were also measured on samples which had previously been irradiated in the range 300° to 650°C.

In this study they report the a-spacing changes saturate at all temperatures in the high fluence irradiations, but the change in c-spacing tends to increase at the higher temperature.

The analysis of the lattice parameter and dimensional changes required certain assumptions and concepts relating to the nature of irradiation damage in graphite. Again, they assumed that polycrystalline graphite considered on a small enough scale can be regarded as a single material, in spite of the complexity of its macroscopic structure, with allowance made for the effect of microscopic defects in the local structure and for the effect of the macroscopic structural variations.

They applied growth equations from Perks and Simmons (1966) to high fluence data and found the most outstanding feature of the growth curves to be their upward trend at high strains. They believed this was due to the generation of porosity.

They described a mechanism for porosity generation during expansion at high fluences. In this scheme, the free growth rate in a particular direction in the graphite may vary from point to point due to local variations of porosity and orientation, and these variations give rise to internal stresses that will be reduced to some extent by creep relaxation. Creep relaxation will suppress the variation of growth rate within the block, but the variations should be apparent on the surface of the specimen. They found the surface of an anisotropic graphite specimen, which was initially optically flat, had roughened. They believe variations of growth rate occur over quite large volumes within an anisotropic graphite.

4.6 Size Effect

Investigators at BNWL (Nightingale and Woodruff, 1964) have reported that some large reactor graphite blocks measured in a reactor apparently contract at a higher rate initially than smaller samples of the same material irradiated in capsule experiments. They reported this effect to be a factor of 2. Gray and Russell (1969) have recently reported data which they claim support the existence of a size effect on the irradiation-induced contraction of nuclear graphite, but the effect is not as large as originally reported by Nightingale and Woodruff. Although the data of Gray and Russell were quite scattered, they considered the magnitude of the observed size effect to be too large to attribute to experimental error.

Gray believes that possibly some factor in addition to size, such as preferred orientation effects or irradiation history, affects the dimensional changes of the large bars.

Horner et al. (1966) have measured graphite struts after irradiation in graphite-moderated reactors in the United Kingdom and compared their dimensional changes with small samples irradiated in capsules. Their results indicate that the dimensional changes in the graphite struts are in agreement with the small encapsulated samples.

4.7 Fabrication Versus Irradiation Effects

Engle (August 1971) prepared and irradiated at 1225°C to fluences of 11.5×10^{21} n/cm^2 a series of molded needle-coke graphites where the coal-tar pitch binder coke was varied between 5 to 14 percent by weight.

The dimensional changes in the c-axis direction were sensitive to the binder-coke fraction, showing decreasing expansion with increasing binder-coke content and going through an optimum at a binder-coke fraction of about 11 wt %. The a-axis direction changes were dependent upon the binder-coke content, showing larger contractions by a factor of 2 when the binder-coke content was high. Volumetric expansion was largest when the binder-coke content was low and smallest at the optimum value of 11 wt %.

Rappeneau et al. (1971) irradiated graphites fabricated from three cokes deliberately chosen for their different properties. The first was a needle coke giving strongly anisotropic properties, the second an isotropic Gilsocoke, and the third an intermediate fibrous coke. The graphitization rates were varied between 50°C/hr and 3300°C/hr. The apparent density of the products decreased as the graphitization rate increased. The true densities decreased as the heating rate increased.

The graphitization rate was shown to influence the micropore structure of the graphites and was believed responsible for the dimensional behavior of these graphites under irradiation.

Graphites graphitized at 50, 200, 500, 2000, and 3300°C/hr were irradiated between 470° and 560°C and to fluences of 5 to 8 x 10^{21} n/cm^2. As the heating rate of graphitization increased, an increase in the contraction rate was observed, especially in the c-axis direction, and the contraction curve minimum moved toward higher fluences.

Markel et al. (1968) prepared two controlled series of graphite specimens, where the graphitization rate was varied in one and the binder was graphitized at temperature intervals in the range 1300° to 2900°C in another. They found that increasing the graphitization rate produced a decrease in the bulk density, but the contraction rate was not affected during irradiation at 550° to 700°C to about 3 x 10^{20} n/cm^2. An increase in contraction rate was found with decreasing processing temperature in the binder coke.

These authors concluded that the binder coke significantly contributes to the graphite irradiation dimensional change when the degree of graphitization of the binder coke is different.

4.8 Summary

There appears to be almost unanimous agreement among the various investigators that volume expansion after turnaround at high temperatures results from pore generation and isotropic graphites with relatively high density and high strength are the most stable. These materials usually have relatively small crystallites, but their high strength offset the crystallite size effect and prevent pore generation which is responsible for the large

volume expansions observed in the weaker more anisotropic graphites. Again there is good agreement that the lower pore generation results from a higher irradiation-induced creep rate in the isotropic materials that allows plastic deformation to relieve stresses. Pyrolytic carbons behave in a like manner.

Dimensional instability appears to be maximized in the range 900° to 1200°C due to high expansion rates. However, some data are available to indicate that above 1200°C the expansion rate decreases again. More work is needed to confirm this observation.

Some progress has been made in sorting out the microstructural and porosity changes that occur at high temperatures and high fluences, but the complexity of reactor graphite structures permits only qualitative interpretations at this time.

Certain relatively large pores or cracks close during densification due to c-axis expansion, while other micropores are generated within or between crystallites. Macroporosity is generated when volumetric expansion begins. Lack of quantitative methods to analyze pore morphology and structure after irradiation continues to hamper studies in this area.

Early models based on thermal expansion and crystallite orientation were successful in predicting dimensional changes at low fluences, but are of little use at high fluences. These models have been updated to conform

to recent data obtained at high temperatures and higher fluences but microstructural and porosity changes continue to complicate the efforts to produce a truly quantitative model.

Limited data are available that attempt to correlate dimensional changes with variations of certain fabrication processes in conventional binder-filler cokes. These studies show the dimensional changes to be sensitive to manipulations of the binder-coke content.

5. THERMAL PROPERTIES

The important thermal properties with respect to reactor design are thermal expansivity and thermal conductivity.

Dimensional tolerances must be met in the initial design and maintained within tolerable limits during the life of the reactor. Thermal stresses in the graphite components during operation and shutdowns are critically dependent upon, among other properties, the thermal expansion coefficient and thermal conductivity of the graphite moderator blocks. Low thermal expansivity and high thermal conductivity values are desirable. Heat is conducted from the fuel to the coolant through the graphite in high-temperature gas-cooled reactor designs, and any adverse changes in the conductivity will affect the fuel operation temperature and the performance of the reactor. Thus, it is critically important that any changes in the thermal properties be minimized and known.

5.1 Thermal Expansivity

In graphite crystals the thermal expansion coefficient parallel to the c-axis, α_c, is large and positive; that in the layer plane, α_a, is small and negative at low temperatures, but becomes positive at about 400°C. Early measurements by a number of investigators on single crystals and later work

on annealed pyrolytic carbon, along with the theoretical analysis of the thermal expansion, have been recently summarized by Reynolds (1968).

The thermal expansion of polycrystalline reactor graphites is usually only a fraction of that of the single crystals. For the volume coefficients α_v, the fraction is usually ~30%. Mrozowski (1956) suggested that the explanation was associated with the porosity and cracks of artificial materials. These are preferentially planar and parallel to the local basal planes, so that they prevent the high c-axis expansion from contributing its full quota to the overall dimensional changes. In the high-density, high-strength graphites which are isotropic, α_v more closely approaches the single crystal value. The linear values in anisotropic graphites are usually anisotropic in a proportion determined by the raw materials and manufacture, the anisotropy being always less than that of the single crystal.

A number of investigators have measured the changes of thermal expansivity in reactor graphites as a function of neutron fluence at elevated temperature and to high fluences (Blackstone et al., 1969; Delle and Vohler, 1971; Engle, August 1971; Engle and Bokros, 1971; Gray and Pitner, 1971; Hankart et al., June and September 1971; Pitner, July 1971). The curves in Figure 9a from BNWL (Helm, 1969) and in Figure 9b from Gulf General Atomic Company (Engle, August 1971) show the changes in anisotropic petroleum-coke graphites. The needle-coke graphites increase with fluence at 1000° to 1200°C up to about 20×10^{21} n/cm^2, except for one needle-coke graphite which did not change. The near-isotropic graphites from the Dragon Project and Gulf General Atomic Company (Blackstone et al., 1969; Engle and Bokros, 1971; Hankart et al., June and September 1971) that have original thermal

expansivity values above those of the needle coke (see Figures 9b and 9c) first increase slightly and then decrease with increasing fluence. The changes in thermal expansivity are small at low fluences while the graphites are densifying; the large increase or decrease accompanies the volume expansions that take place at high fluences after volumetric turnaround (see Figures 3 through 6).

Thermal expansivity changes of high-density, high-strength graphites, which are isotropic and which have large unirradiated values ($\sim 7 \times 10^{-6}$ °C^{-1}), are shown in Figure 9d at 500° to 1300°C (Pitner, October 1971). At 1000° to 1100°C, the values decrease rapidly with fluence until they reach values of about 2×10^{-6} °C^{-1}. The changes at 1200° to 1300°C are less than those at the intermediate temperature.

Taken together, the data in Figures 9a through 9d show the thermal expansivities of anisotropic graphites with low unirradiated thermal expansivity values increase, whereas those that are isotropic with high unirradiated values decrease.

Fitzer et al. (1968) have also observed a decrease in isotropic Gilsocarbon graphites at 1200°C. Helm (1969) has found the same effect on a number of isotropic graphites. Nettley and Martin (1966) also found that initially the linear thermal expansion coefficients of the isotropic graphites increased with fluences, but at high fluences decreased again during irradiation at 500° to 750°C.

Delle and Vohler (1971) have measured changes in thermal expansivity of petroleum-coke or pitch graphites. Below 600°C the coefficient of linear thermal expansion first increased up to 30% and remained high with increasing fluence. Above 600°C the thermal expansion of these materials decreased with increasing fluence. They found that Gilsocarbon graphites showed large decreases in thermal expansivity.

The thermal expansion coefficients of the hot-worked graphite and massive pyrolytic carbon samples in the two principal directions (Price, 1969) are also of interest in understanding the changes in the reactor graphites (see Figure 10). At 750° to 800°C the expansion coefficient of the hot-worked graphite parallel to the hot-working axis (c-axis direction) showed a gradual increase with neutron exposure, rising from 15 x 10^{-6} $°C^{-1}$ (unirradiated) to 17 x 10^{-6} $°C^{-1}$ at 1.8 x 10^{21} n/cm^2. The coefficient remained unchanged perpendicular to the axis. However, at 1200°C the expansion coefficient parallel to the axis showed an initial rise, passed through a maximum of 19 x 10^{-6} $°C^{-1}$ at 2.4 x 10^{21} n/cm^2, and then fell to about half its original value by 11.6 x 10^{21} n/cm^2 (see Figure 10). In the perpendicular direction it increased from 1 x 10^{-6} °C to 2 x 10^{-6} $°C^{-1}$ over the same neutron exposure. The massive pyrolytic carbon behaved somewhat differently. At 750° to 800°C the thermal expansion coefficient was unchanged by the irradiation. No significant changes were observed in the thermal expansion coefficients of pyrolytic graphite at 500° to 750°C as determined by Nettley and Martin (1966). At 1250°C perpendicular to the deposit it increased rapidly from 25 to 27 x 10^{-6} $°C^{-1}$ and showed no sign of a subsequent decrease, despite the formation of delamination cracks. Parallel to the deposit there was no significant change.

Thermal expansivity changes drastically in most reactor graphites during high-temperature irradiation, the changes corresponding with the onset of volumetric expansion. The changes are not uniform among the graphites; the weak anisotropic materials with initially low coefficients generally increase, whereas the strong isotropic materials with initially high coefficients decrease. No theoretical analyses have been undertaken to explain the thermal expansivity changes. It had generally been assumed that thermal expansivity would increase after basal plane cracks, which accommodate c-axis expansion, were exhausted. This idea may have to be revised in light of the current data.

5.2 Thermal Conductivity

Thermal conductivity of reactor graphite is reduced during fast-neutron irradiation at elevated temperatures (Delle and Vohler, 1971; Engle and Koyama, 1971; Kelly and Brocklehurst, 1971; Nettley and Martin, 1966; Taylor et al., 1969). Thermal conductivity measurements have been obtained on a number of materials as a function of fluence at 300° to 1200°C to fluences of 2×10^{22} n/cm^2 (Engle and Koyama, 1971; Helm, 1969; Taylor et al., 1969). Data representative of the changes that are characteristic of reactor graphites are shown in Figure 11 at 625°, 1000°, 1200° and 1400°C to high fluences. The effect of irradiation on thermal conductivity as a function of measuring temperature is shown in Figure 12 for reactor graphites irradiated at 2 to 4×10^{21} n/cm^2 at 300° to 1500°C (Engle and Koyama, 1968).

The data show that thermal conductivity, measured at room termperature, decreases rapidly with fluence, saturates, and then decreases again with the onset of breakaway expansion. There is also a strong temperature effect; conductivity degradation was reduced with increasing irradiation temperature.

Taylor et al. (1969) have analyzed the behavior of the thermal conductivity changes in highly annealed pyrolytic carbons in the range 30° to 450°C to 5 x 10^{20} n/cm^2 and reactor graphites at 200° to 1350°C to 5 x 10^{21} n/cm^2 in terms of the lattice defects that cause dimensional changes. These authors concluded that thermal conductivity changes are due to submicroscopic clusters, vacancies in the lattice, and vacancy loops, and that interstitial loops and collapsed vacancy lines, which are responsible for dimensional changes, are insignificant.

They (Taylor et al., 1969) indicate that thermal conductivity changes of reactor graphites, however, are larger at irradiation temperatures above 650°C than can be accounted for by vacancy content estimated from lattice parameter changes. They have estimated room temperature thermal conductivity changes by the analysis of crystallite dimensional changes in reactor graphites at 650° to 1350°C to 4 x 10^{21} n/cm^2 and found that the vacancy loops responsible for thermal degradation increase both in size and separation with increasing irradiation temperature. This is in agreement with low fluence data observed by other investigators (Blackstone et al., 1969; Delle and Vohler, 1971; Engle and Koyama, 1968; Engle and Koyama, 1971) and may explain the smaller fractional changes in conductivity with increasing irradiation temperature.

Engle and Koyama (Engle, October 1971; Engle and Koyama, 1971) now have data on reactor graphites irradiated to high fluences in the range 500° to 1400°C (see Figure 11) and have found the same temperature effect with both anisotropic and isotropic reactor graphites. Taylor et al. (1969) concluded that after the initial rapid degradation of conductivity which saturates at about 3 to 5 x 10^{21} n/cm^2, further changes in conductivity would not occur until large expansions begin above 1 x 10^{22} n/cm^2. Comparison of thermal conductivity changes in Figure 11 with dimensional changes supports the conclusion by Taylor et al. (1969) that crystal defects responsible for dimensional changes do not correlate with thermal conductivity changes.

Engle and Koyama (1971) in annealing their graphites found the following. Recovery of conductivity was slower in Gilsocarbon graphite than in needle-coke graphites after irradiation to about 3 x 10^{21} n/cm^2 at 1200°C under identical annealing conditions of 1500°C. After irradiation to 8 x 10^{21} n/cm^2 at 1200°C, recovery of conductivity was even more difficult when the same materials were annealed at 1700°C, and the fractional changes remained large. It should be noted here that no increase in fractional conductivity change took place in these graphites between 3 and 8 x 10^{21} n/cm^2. Taylor et al. (1969) have calculated a decrease in the spacing between vacancy loops or an increase in loop population in reactor graphites between 1 and 4 x 10^{21} n/cm^2 at 1350°C, which would indicate a steady reduction of thermal conductivity over this fluence range. The large interstitial loops, which cause dimensional change, must certainly grow during the fluence region where the conductivity is not changing, because the crystallites continue to distort. Taylor's calculations indicate that the vacancy loop size remains constant and that the population may be leveling off at 4 x 10^{21} n/cm^3.

In a later paper, Kelly and Brockelhurst (1971) show the conductivity degradation to saturate at a fluence of about 5×10^{21} n/cm^2. Kelly and Brockelhurst (1971) indicate that scattering sites due to submicroscopic clusters in graphite crystals irradiated at 150°C can be removed with a 1900°C anneal by aggregation into interstitial loops. Samples irradiated at higher temperatures recover much less. At irradiation temperatures above 1000°C, it is doubtful whether the population of submicroscopic clusters or vacancies remains due to enhanced thermal effects; thus, thermal degradation may be due only to vacancy loops. At higher fluences the vacancy loops may couple with the growing interstitial clusters and thus annealing or annihilation may be more difficult than at lower fluences.

A further degradation in thermal conductivity with irradiation to still higher fluences ($\sim 2 \times 10^{22}$ at 1200°C), where the graphites expand rapidly and become highly porous, has been observed (Delle and Vohler, 1971; Engle and Koyama, 1971).

It is tempting to assign this final degradation in conductivity to the formation of porosity. However, in two graphites taken to 2×10^{22} n/cm^2 (Engle and Koyama, 1971), the thermal conductivity was extremely low and nearly identical in both samples, but there was a factor of 3 difference in their volume expansion.

Considerable progress has been made in the theory of the thermal conductivity of graphites through observations on highly annealed pyrolytic carbons. Defects which cause thermal conductivity degradation during low

to intermediate irradiation temperatures have been identified up to limited fluences. While considerable dimensional data are available in the range 800° to 1300°C to 2 x 10^{22} n/cm^2, the thermal conductivity data are not as abundant. Several investigators have thermal conductivity data extending into this range and the general behavior has been observed; however, there has been no systematic examination of thermal conductivity changes. Additional experimental and theoretical work is required at high fluences.

6. MECHANICAL PROPERTIES

6.1 Introduction: The Stress-Strain Relationship for Unirradiated Graphite

Conventional reactor-grade graphites before irradiation exhibit a nonlinear stress-strain curve, which is sensitive to past history and exhibits a hysteresis effect upon load cycling. Moreover, the tensile strain-to-failure is only about 0.25%. Clearly, in view of the discussion on bulk and crystallite dimensional changes, an irradiation-induced mechanism must exist to relieve the internally developed stresses, or graphite would quickly disintegrate. Before discussing radiation effects, it is advantageous to quickly review the mechanical behavior of unirradiated graphite. The factors involved in the unirradiated material provide some qualitative explanation for the irradiation-induced phenomena.

The general behavior of uniaxially stressed graphite is indicated in Figure 13. Upon applying a stress σ, the graphite strains nonlinearly, as indicated by the curve AB. If the maximum stress σ_m is not too close to the ultimate strength, the material relaxes along the curve BC, leaving a residual strain ε_o. Reloading to a stress less than σ_m produces the curve CD, which relaxes linearly back along the line DC. Further loading to a stress greater than σ_m produces the curve CDE, which becomes an extension (EF) of the original curve AB.

A number of semiempirical equations have been suggested to fit the behavior of Figure 13. The simplest is that recommended by Jenkins (1963), for which he has provided a semiquantitative theoretical basis. The original loading curve AB is fitted closely by

$$\varepsilon = A\sigma + B\sigma^2$$

and the unloading curve BC by

$$\varepsilon = \varepsilon_m - A(\sigma_m - \sigma) - \frac{1}{2}B(\sigma_m - \sigma)^2$$

Upon reloading, the curve CDE is given by

$$\varepsilon = \varepsilon_o + A\sigma + \frac{1}{2}B\sigma^2$$

with the permanent set

$$\varepsilon_o = \frac{1}{2}B\sigma_m^2$$

The two coefficients A and B are related (Jenkins et al., 1965) to crystallite size and orientation. The coefficient A in a particular direction depends upon the crystal shear stiffness C_{44} as well as the density of dislocations and their pinning characteristics, whereas B depends on the generation of new dislocations. Thus, a picture emerges of an individual crystallite plastically shearing as dislocations are unpinned by the applied stress, eventually piling up at the crystallite boundaries, to provide a restraining

back stress. Mason and Knibbs (1967) extended this work to further delineate the effect of temperature and crystal size. In particular, they point out that at temperatures above 300°C the increase in Young's modulus with temperature can be explained by closure of voids due to the anisotropic crystallite expansions, thus effectively locking the material together.

We thus have a fairly satisfactory qualitative, and indeed semiquantitative, theoretical basis to account for the stress-strain characteristics of unirradiated graphite, involving dislocation motion and pinning as well as the microporosity of the materials.

6.2 Strength of Irradiated Graphite

Very little work has been done on measuring the strength of reactor graphites after high-temperature irradiation. Taylor et al. (1967) observed an increase in tensile strength of reactor graphites of up to 100% irradiated at 150°C to low fluences. Krefeld et al. (1971) measured changes in tensile strength on Gilsocarbon graphites and petroleum coke graphites at 1200°C to a fluence of about 5×10^{20} n/cm^2. This experiment was treated statistically and they reported that a graphite with a high mean unirradiated strength may have a higher risk of failure at some stress below the mean fracture stress after irradiation than one of lower mean strength. This is interpreted to mean that variations of the mean strength due to irradiation are not indicative of the actual risk of failure. This result if confirmed on a wider variety of graphites could be disturbing since it is generally believed that during densification at low fluences strength increases in reactor graphites.

No systematic data were uncovered on strength measurements of graphites after large expansion at high fluences. Pitner (October 1971) mentions the testing of a single high-density high-strength isotropic graphite sample after irradiation at 1050°C and 1.5×10^{22} n/cm^2. On this sample the tensile strength increased by a factor of about 2. However, due to the excellent stability of this material, the expansion was not large at such a high fluence.

The strength of graphite, or more specifically the changes in the probability of failure of graphites after high-temperature, high-fluence irradiation, is of critical importance to reactor designs, and considerably more work is needed in this area.

6.3 Young's Modulus of Irradiated Graphite

Irradiation at temperatures from just above liquid nitrogen to the highest yet studied has shown an immediate increase in the Young's modulus. The effect quickly saturated and only minor dependence on fluence or temperature was subsequently observed. It is generally accepted that the first rapid increase is due to pinning of dislocations by radiation-induced defects, and that these are probably di-interstitials or larger configurations (Goggin, 1963). The saturated value is assumed to represent complete pinning, and subsequent temperature dependence attributable to the crystal shear constant or to thermal unpinning of a small fraction of the dislocations (Summers et al., 1966).

In the last 3 years, information at higher temperatures and much greater fluences has become available. The data are not entirely consistent, and much more remains to be done before general conclusions can be drawn. It is apparent, however, that the situation is much more complex than the early data at low temperatures and fluences implied. The new information was obtained by Battelle Northwest Laboratory (Pitner, July 1971) and the Dragon Project (Hankart et al., June and September 1971). The Battelle group admit to considerable uncertainties in temperature and measure the modulus by sonic resonance. The Dragon investigators obtain the modulus from the stress-strain curve. Much of the Battelle data is so scattered that trends of modulus versus fluence are not discernable. These differences in technique and resolution may account at least in part for the lack of consistency in data on similar graphites.

The highest fluence data is on an anisotropic graphite (Pitner, July 1971), a conventionally formed graphite based on acicular coke (see Figure 14). The curves are not too dissimilar to earlier data indicating simple saturation, although there is a hint of an inflection point at the highest fluences, around 2×10^{22} n/cm^2. These may be compared with the Dragon Project data (Hankart et al., June and September 1971), on experimental acicular-coke graphites (Figure 15), for which the inflection points occur near 5×10^{21} n/cm^2 followed by a maximum.

Isotropic graphites conventionally formed are represented by Gilsocarbon based graphite (Hankart et al., June and September 1971), shown in Figure 16. Although not indicated in the figure, data at 900°C exist to

1.3×10^{22} n/cm^2 and demonstrate a maximum modulus change of $\Delta E/E = 150\%$ at 1.0×10^{22}. The rather subtle differences between the behavior of the anisotropic and isotropic graphites are worth noting. The effects are less dramatic and more delayed in the more isotropic material.

Some data are also available on a high-density, high-strength graphite (Pitner, October 1971) obtained at Battelle (Figure 17). In view of the inconsistencies exhibited by the Battelle and the Dragon data, it is not possible to state that the more dimensionally stable isotropic graphites are also more modulus-stable.

The experimental results hardly justify a serious attempt at theoretical justification. One is nevertheless tempted to hypothesize a rationalization: after the dislocation pinning process is completed, a further hardening of the material occurs as crystal-to-crystal interlocking occurs (Reynolds, 1965; Thrower and Reynolds, 1967). The crystal interlocking eventually gives rise to direct pore-generation or fracture (Summers et al., 1966; Taylor et al., 1967), which leads to the apparent decrease in modulus. It remains for the future to establish these hypotheses and to unravel the behavior of the Young's modulus as measured sonically or from the stress-strain curve (Taylor and Kline, 1970).

6.4 Radiation-Induced Creep

It is somewhat surprising that a relatively obscure property such as creep has emerged as one of the critical properties of nuclear graphite.

Thermally induced creep is of significance only at temperatures in excess of 2000°C (Reynolds, 1968). Yet in a neutron-irradiation environment, creep becomes an important phenomenon at temperatures as low as 300°C. Graphite will normally withstand strains of only 0.1 to 0.3% before fracture, but will take at least ten times this strain in a radiation field. In view of the irradiation-induced distortion and its temperature dependence, graphite would rapidly disintegrate without this relaxation process. The creep characteristics are a dominant stress-relaxation parameter in the reactor designer's analysis (Head and Sockalingam, 1968; Scott and Eatherly, 1970).

Irradiation-induced creep takes place in two stages, the first (primary) being a reversible process which is quickly exhausted, and for practical purposes may be considered a pseudoelastic process. This is followed by an irreversible steady-state secondary creep, whose rate is linearly dependent on fluence and stress.

The creep problem is further confused by the change in Young's modulus, equivalent in itself to a permanent set under irradiation. Losty (1966), who did the pioneering work on creep, argues persuasively that the creep coefficient should be defined so that the material system does no external work, and this viewpoint has been uniformly accepted in defining the creep coefficient (Simmons, 1962).

The early work on creep was performed on springs and constrained-geometry samples. The first clearcut experiments designed to produce uniform stress fields constant in time were performed by Kennedy (1967), whose

results at low temperature (>400°) were inconsistent with those of Losty. This discrepancy has been left unresolved, and need concern us only as it leads to doubt for the higher temperature data. Fortunately, the higher temperature situation has been resolved in the last 3 years.

The first clearcut resolution of the problem was furnished by Platonov et al. (1969), whose data are superimposed upon Kennedy's in Figure 18. Subsequently, the Dragon Project (Blackstone et al., 1969), have further substantiated the high-temperature results and extended them from ∿900° to ∿1200°C (Figure 19).

The available data on secondary creep coefficients leave many questions unanswered. The range of graphite structures covered is limited. From analogy with thermally induced high-temperature creep, one would expect orientation and density parameters to enter into the functional dependence of the secondary creep coefficient. No clearcut demonstration has been made, although some indication of an inverse relationship between Young's modulus and creep coefficient has been suggested (Brocklehurst and Brown, 1969; Kennedy, 1966).

Theoretical aspects of irradiation creep in graphite have been discussed by Kelly and Brocklehurst (1970). They presented a theoretical model for irradiation creep in which basal shear is the dominant deformation mode that predicts an irradiation creep rate inversely proportional to the initial Young's modulus of the sample, in good agreement with several experiments. The irradiation-induced shear strain during transient creep is believed to

be caused by the removal of pinning points for basal dislocations. The mechanism for secondary creep is not yet established. Suggestions include internal yielding resulting from irradiation-induced crystal strains, the diffusion of interstitials in the high stress gradients present at the tips of basal plane microcracks, grain boundary sliding, de-interleaving of crystals, and the restraint of c-axis growth. Each of these mechanisms is either inconsistent with some part of the experimental observations or has not been quantified to the point where useful comparisons with the data can be made.

7. CONCLUSIONS AND FUTURE TRENDS

A complete understanding of the irradiation behavior or reactor graphites at high temperatures and high fluences has not been attained, but a number of significant advances have been made during the past 6 to 7 years. The irradiation data have been extended to fluences of 4×10^{22} n/cm^2 and temperatures into the range 900° to 1400°C. The irradiation of reactor graphites has been paralleled by similar studies on as-deposited pyrolytic carbons and annealed pyrolytic carbons which approach single crystals in structure.

New insights have been made into the mechanism of irradiation damage to crystallites through electron microscopy and the nature and mobility of defects in single crystals is now better understood. However, direct observation of the neutron-induced defects in reactor crystallites continues to be retarded by experimental difficulties in sample preparation and the poor diffraction qualities of the reactor graphites. Progress has been made in analyzing dimensional changes and certain property changes such as thermal conductivity and Young's modulus in reactor graphites in terms of defects observed in the annealed pyrolytic carbons and single crystals, but again the direct observations of damage in reactor graphite crystallites would be helpful to confirm these interpretations. Microstructural changes in reactor graphites have been measured and explained, but only in qualitative terms. Better quantitative experimental techniques, to measure crystallite and pore morphology changes, are required in this area.

The effect of irradiation temperature on the dimensional change rate of reactor graphites in the range 900° to 1400°C needs to be clarified. There appears to be a temperature range from 900° to 1200°C where structural degradation is severe, whereas above about 1200°C lower dimensional change rates have been reported. However, data are not abundent above 1200°C and anomolies exist. More experiments are needed at 900° to 1400°C and improvements in thermometry and dosimetry above 1200°C will be required.

Several novel high-temperature, high-strength isotropic graphites have come under study during the past 6 to 7 years and were shown to have improved dimensional stability over conventional graphites manufactured with anisotropic petroleum-based cokes. Unfortunately, at present, these materials have limited use in large commercial high-temperature gas-cooled power reactors due to limitations in production size and the high costs of processing. While economic design of power reactors appears feasible from conventional materials, it is encouraging to note that improvements are possible and further development of economical isotropic graphites for commercial power reactors should be encouraged.

High-temperature gas-cooled reactors have now become a commercial product. Each reactor will utilize about 1500 tons of high-purity nuclear-grade graphite in the form of large moderator blocks. Future improvements in design of the reactors may require the graphites to remain in the reactor environment to higher fluences and to operate at higher temperatures and, thus, continued efforts will be needed to obtain commercial graphites with improved irradiation stability.

ACKNOWLEDGMENTS

The authors are grateful to R. J. Price who read the manuscript and made many helpful comments. This paper was prepared under Contract AT(04-3)-167, Project Agreement No. 12.

LITERATURE

Bacon, G.E., 1956, J. Appl. Chem., 6, 447.

Blackstone, R., Graham, L.W., Everett, M.R., Delle, W., 1969, in Radiation Damage in Reactor Materials, Vol. II, IEAE, Vienna, 543.

Blackstone, R., Krefeld, R., Everett, M.R., Delle, W.W., 1971, 10th Biennial Conference on Carbon, Paper No. RD-126, Bethlehem, Pennsylvania.

Bokros, J.C., 1969, in Chemistry and Physics of Carbon, Ed. P.L. Walker (Marcel Dekker, New York) 1.

Bokros, J.C., Guthrie, G.L., Schwartz, A.S., 1968, Carbon, 6, 55.

Bokros, J.C., Koyama, K., 1970, J. Appl. Phys., 41, 2146.

Bokros, J.C., Price, R.J., 1967, Carbon, 5, 301.

Bokros, J.C., Stevens, D.W., 1971, Carbon, 9, 19.

Bokros, J.C., Stevens, D.W., Aikens, R.J., 1971, Carbon, 9, 439.

Brocklehurst, J.E., Brown, R.G., 1969, Carbon, 7, 487.

Cox, J.H., Helm, J.W., 1969, Carbon 7, 319.

de Halas, D.R., 1962, in Nuclear Graphite, Ed. R.E. Nightingale (Academic Press, New York) 195.

de Halas, D.R., Yoshikawa, H.H., 1962, in Proceedings of the Fifth Carbon Conference, 249.

Delle, W.W., Vohler, O., 1971, 10th Biennial Conference on Carbon, Paper No. RD-129, Bethlehem, Pennsylvania.

Eatherly, W.P., 1969, in USAEC Report ORNL-4449, Oak Ridge National Laboratory.

Eatherly, W.P., Kennedy, C.R., 1971, in USAEC Report ORNL-4728, Oak Ridge National Laboratory.

Engle, G.B., 1970, Carbon, 8, 485.

Engle, G.B., August 1971, Carbon, 9, 383.

Engle, G.B., October 1971, Carbon, 9, 539.

Engle, G.B., Bokros, J.C., 1971, 10th Biennial Conference on Carbon, Paper No. RD-106, Bethlehem, Pennsylvania.

Engle, G.B., Koyama, K., 1968, Carbon, 6, 455.

Engle, G.B., Koyama, K., 1971, 10th Biennial Conference on Carbon, Paper No. RD-108, Bethlehem, Pennsylvania.

Engle, G.B., Pitner, A.L., 1970, USAEC Report GA-9973, Gulf General Atomic.

Fitzer, E., Fritz, W., Delle, W., 1968, Carbon, 6, 273.

Goggin, P.R., 1963, Nature, 199, 367.

Gray, W.J., Pitner, A.L., 1971, Carbon, 9, 699.

Gray, W.J., Russell, A., 1969, private communication to G.B. Engle.

Hankart, L.J., Everett, M.R., Blackstone, R., June 1971, Dragon Project Report DPTN/155.

Hankart, L.J., Everett, M.R., Blackstone, R., September 1971, Dragon Project Report DPTN/155 (Supplement).

Head, J.L., Sockalingam, K.C., 1968, J. Mech. Eng. Sci, 10, 402.

Heerschap, M., Schüller, E., 1969, Carbon, 7, 624.

Helm, J.W., 1964, Carbon, 1, 435.

Helm, J.W., 1969, USAEC Report BNWL-1056A, Battelle Northwest Laboratory.

Henson, R.W., Perks, A.J., Simmons, J.A.E., 1968, Carbon, 6, 789.

Hinman, G.W., Haubold, A., Gardner, J.O., 1970, Carbon, 8, 341.

Horner, P., Phelps, B.A., Uglow, A.G., 1966, J. Nucl. Mater., 19, 93.

Jenkins, G.M., 1963, Phil. Mag., 8, 903.

Jenkins, G.M., Williamson, G.K., Barrett, J.T., 1965, Carbon, 3, 1.

Kaae, J.L., Bokros, J.C., Stevens, D.W., 1971, Gulf General Atomic Report GA-10882.

Kaae, J.L., Stevens, D.W., Bokros, J.C., 1971, 10th Biennial Conference on Carbon, Paper No. RD-122, Bethlehem, Pennsylvania.

Kelly, B.T., 1966, Phil. Trans. Roy. Soc., 37, 260.

Kelly, B.T., 1969, in Chemistry and Physics of Carbon, Ed. P.L. Walker (Marcel Dekker, New York).

Kelly, B.T., Brocklehurst, J.E., 1970, Third Conference on Industrial Carbon and Graphite.

Kelly, B.T., Brocklehurst, J.R., 1971, Carbon, 9, 783.

Kennedy, C.R., 1966, in USAEC Report ORNL-3885, Oak Ridge National Laboratory.

Kennedy, C.R., 1967, in USAEC Report ORNL-4170, Oak Ridge National Laboratory.

Kennedy, C.R., 1969, in USAEC Report ORNL-4396, Oak Ridge National Laboratory.

Kennedy, C.R., 1970, in USAEC Report ORNL-4548, Oak Ridge National Laboratory.

Krefeld, R., Linkenheil, G., Meeldijk, J., 1971, 10th Biennial Conference on Carbon, Paper No. RD-114, Bethlehem, Pennsylvania.

Markel, R.W., Parker, W.E., Cox, J.H., 1968, Carbon, 6, 349.

Losty, H.H.W., 1966, in Proceedings of the Fourth Carbon Conference, p. 593.

Mason, I.B., Knibbs, R.H., 1967, Carbon, 5, 493.

Mrozowski, S., 1956, in Proceedings of the 1st and 2nd Carbon Conference, p. 31.

Nettley, P.T., Martin, W.H., 1966, Met. Soc. Conf., 42, 29.

Nightingale, R.E., 1962, Nuclear Graphite (Academic Press, New York).

Nightingale, R.E., Woodruff, E.M., 1964, Nucl. Sci. Eng., 19, 390.

Overholser, L.G., 1969, in USAEC Report ORNL-4396, Oak Ridge National Laboratory.

Perks, A.J., Simmons, J.H.W., 1966, Carbon, 4, 85.

Perry, A.M., Jenkins, J.D., 1967, USAEC Report ORNL-4191, Oak Ridge National Laboratory.

Petrosyants, A.M., 1969, Atomnaya Energiya, 27, 263.

Pitner, A.L., July 1971, USAEC Report BNWL-1540, Battelle Northwest Laboratory.

Pitner, A.L., October 1971, Carbon, 9, 637.

Platinov, P.A., et al., 1969, in Radiation Damage in Reactor Materials.

Price, R.J., 1969, 9th Biennial Conference on Carbon, Paper No. RD-11, Boston College, Massachusetts.

Price, R.J., Bokros, J.C., 1965, J. Appl. Physi., 36, 1897.

Price, R.J., Bokros, J.C., 1967, Carbon, 5, 73

Rappeneau, J., Yvars, M., Mottet, P., 1971, 10th Biennial Conference on Carbon, Paper No. RD-130, Bethlehem, Pennsylvanis.

Reynolds, W.N., 1965, Phil. Mag., 11, 357.

Reynolds, W.N., 1966, in Chemistry and Physics of Carbon, Ed. P.L. Walker (Marcel Dekker, New York).

Reynolds, W.N., 1968, Physical Properties of Graphite (Elsevier, New York).

Scott, D., Eatherly, W.P., 1970, Nucl. Appl. Technol., 8, 179.

Simmons, J.H.W., 1959, in Proceedings of the 3rd Carbon Conference, p. 559.

Simmons, J.H.W., 1961, UKAEA Report AERE-R3883.

Simmons, J.H.W., 1965, Radiation Damage in Graphite (Pergamon Press, New York).

Simmons, J.H.W., 1971, 10th Biennial Conference on Carbon, Paper No. 103, Bethlehem, Pennsylvania.

Summers, L., Walker, D.C.B., Kelly, B.T., 1966, Phil. Mag., 14, 317.

Sutton, A.L., Howard, V.C., 1962, J. Nucl. Mater., 7, 58.

Taylor, R.E., et al., 1967, Carbon, 5, 519.

Taylor, R.E., Kelly, B.T., Gilchrist, K.E., 1969, J. Phys. Chem. Solids, 30, 2251.

Taylor, R.E., Kline, D.E., 1970, in Chemistry and Physics of Carbon, Ed. P.L. Walker (Marcel Dekker, New York).

Thrower, P.A., October 1968b, Phil. Mag., 18, 697.

Thrower, P.A., October 1968a, Carbon, 6, 687.

Thrower, P.A., 1969, in Chemistry and Physics of Carbon, Ed. P.L. Walker (Marcel Dekker, New York).

Thrower, P.A., May 1971, Carbon, 9, 265.

Thrower, P.A., July 1971, 10th Biennial Conference on Carbon, Paper No. RD-104, Bethlehem, Pennsylvania.

Thrower, P.A., Reynolds, W.N., 1967, Phil. Mag., 16, 189.

Turnbull, J.A., Stagg, M.S., 1969, Phil. Mag., 14, 1049.

Walker, P.L., Ed., 1966, 1969, Physics and Chemistry of Carbon (Marcel Dekker, New York).

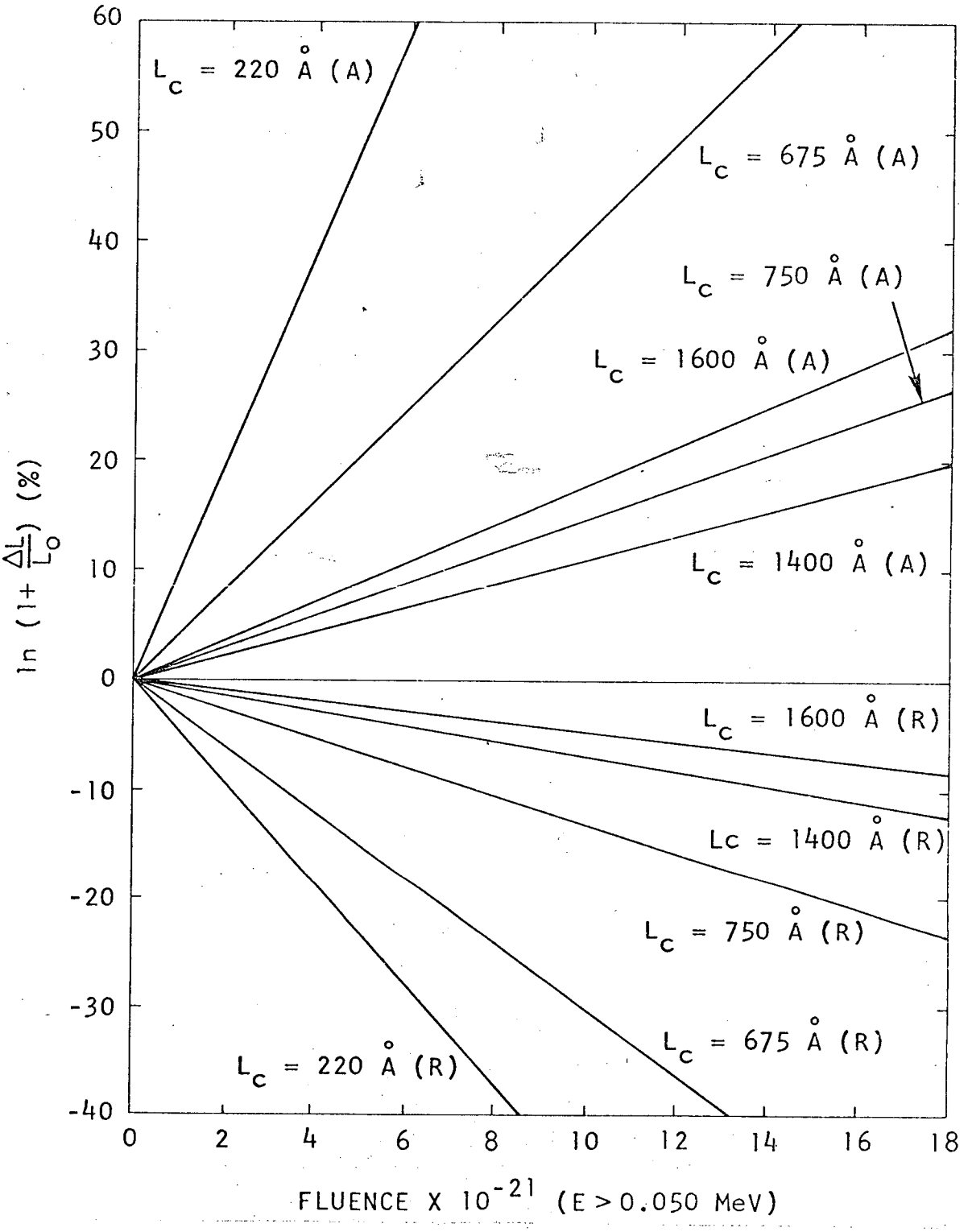

Fig. 1. Dimensional changes in annealed massive pyrolytic carbon irradiated at 1225° to 1300°C (Price, 1969)

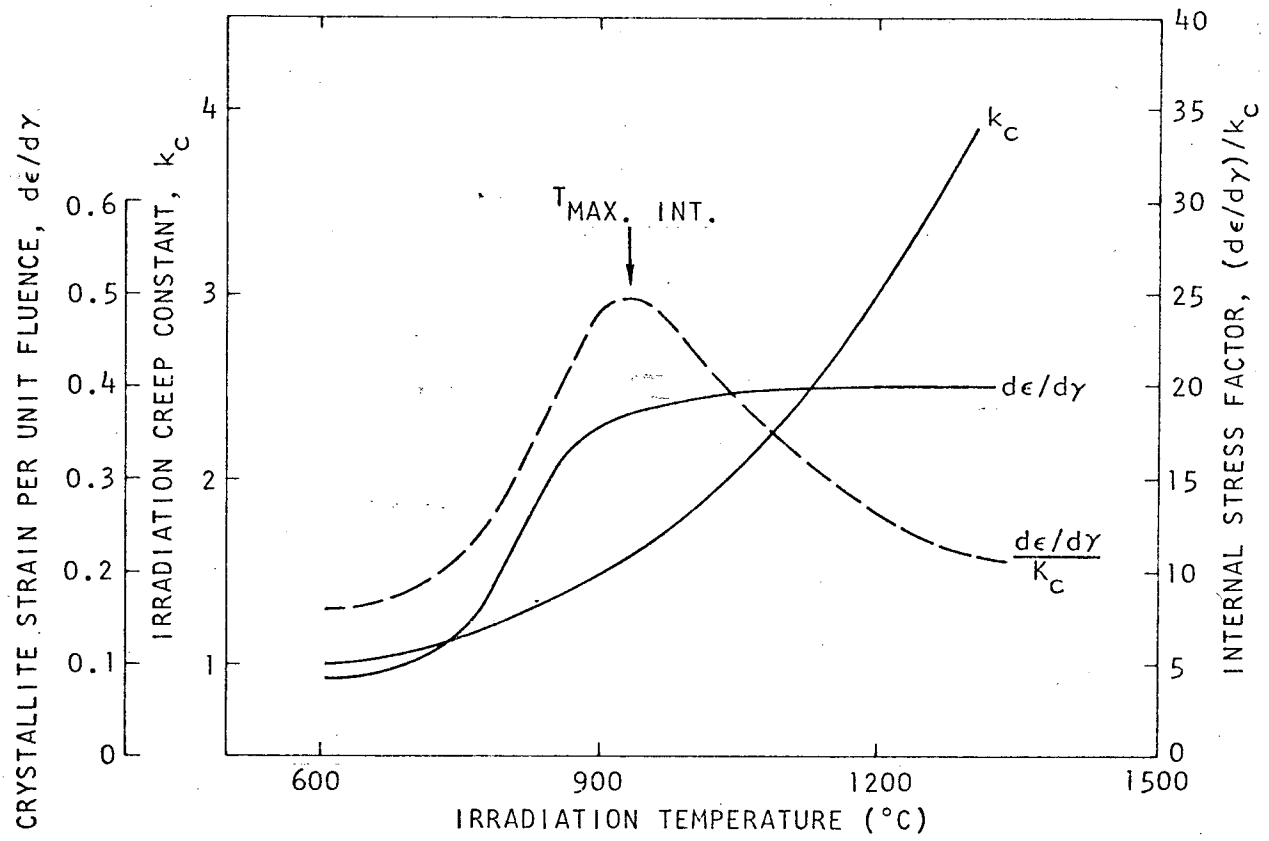

Fig. 2. Irradiation-induced crystallite strain rate, dε/dγ; creep constant, k_c; and internal stress factor $(d\epsilon/d\gamma)/k_c$, for high-temperature isotropic carbons. The data illustrate the factors that lead to a $T_{max.\ int.}$. All units are arbitrary (Engle and Bokros, 1971; Kaae, Bokros, and Stevens, 1971)

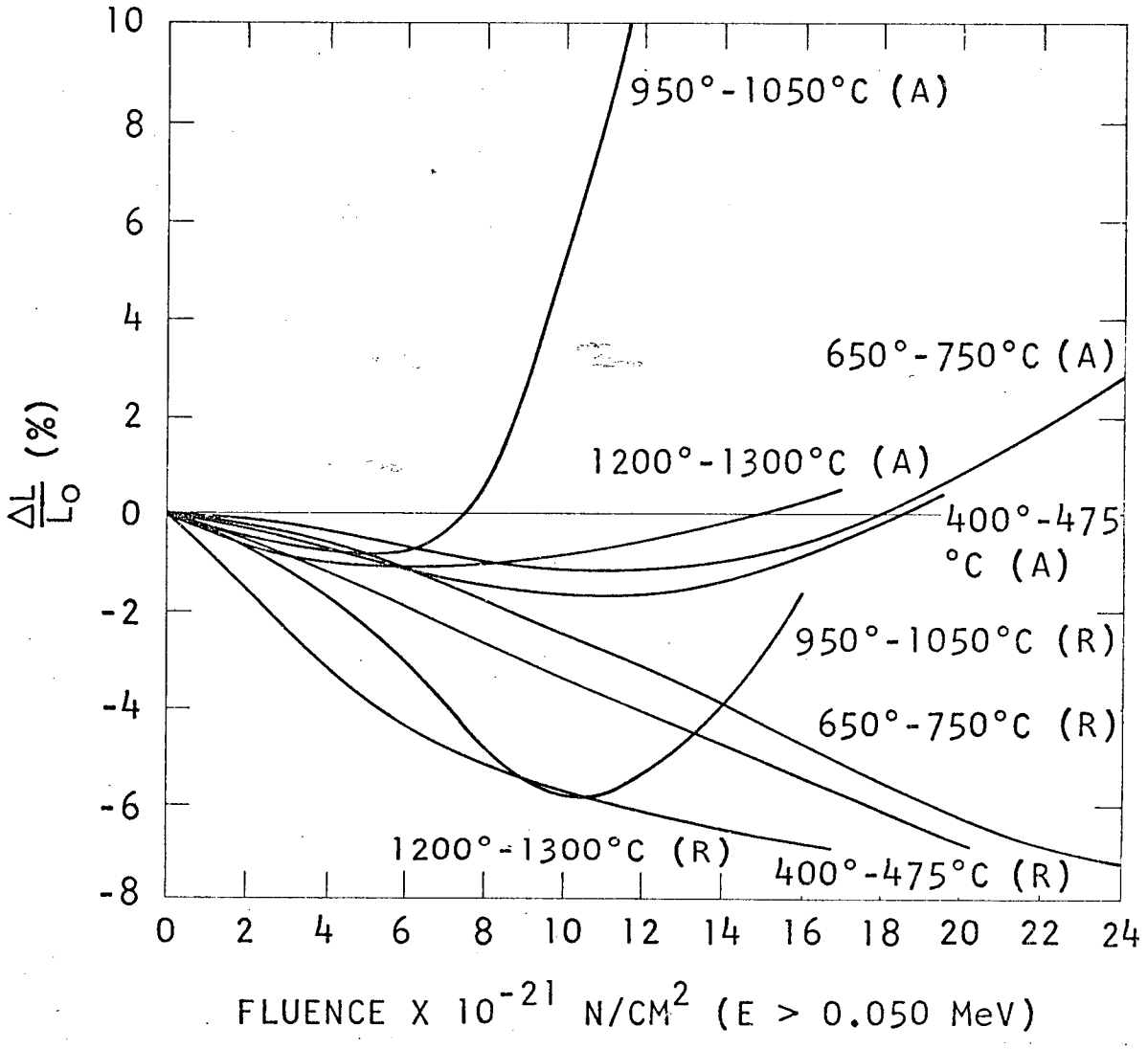

Fig. 3. Dimensional changes versus fluence of anisotropic graphites (a) Gray and Pitner (1971), Cox and Helm (1969)

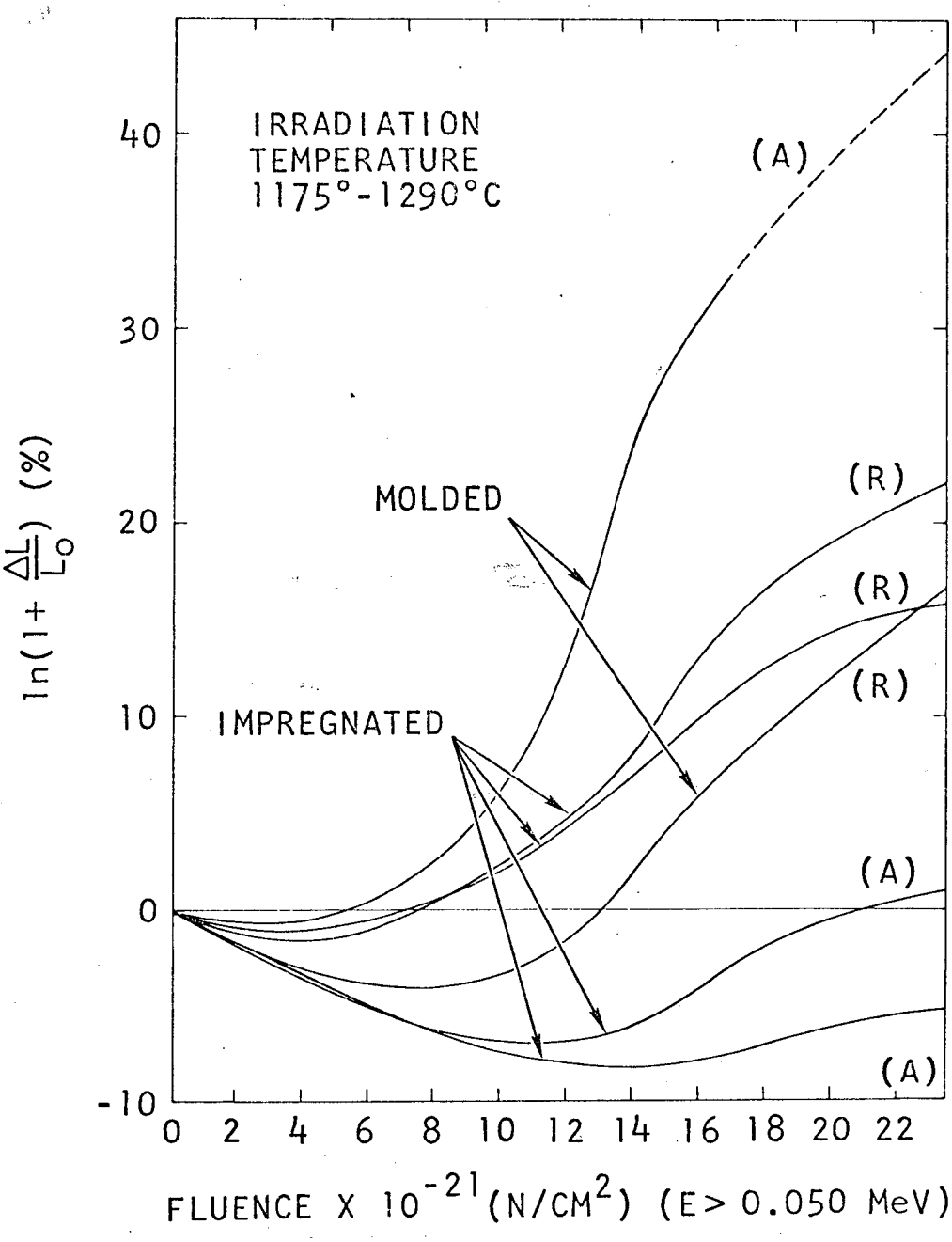

Fig. 3. Dimensional changes versus fluence of anisotropic graphites (b) Engle and Bokros (1971)

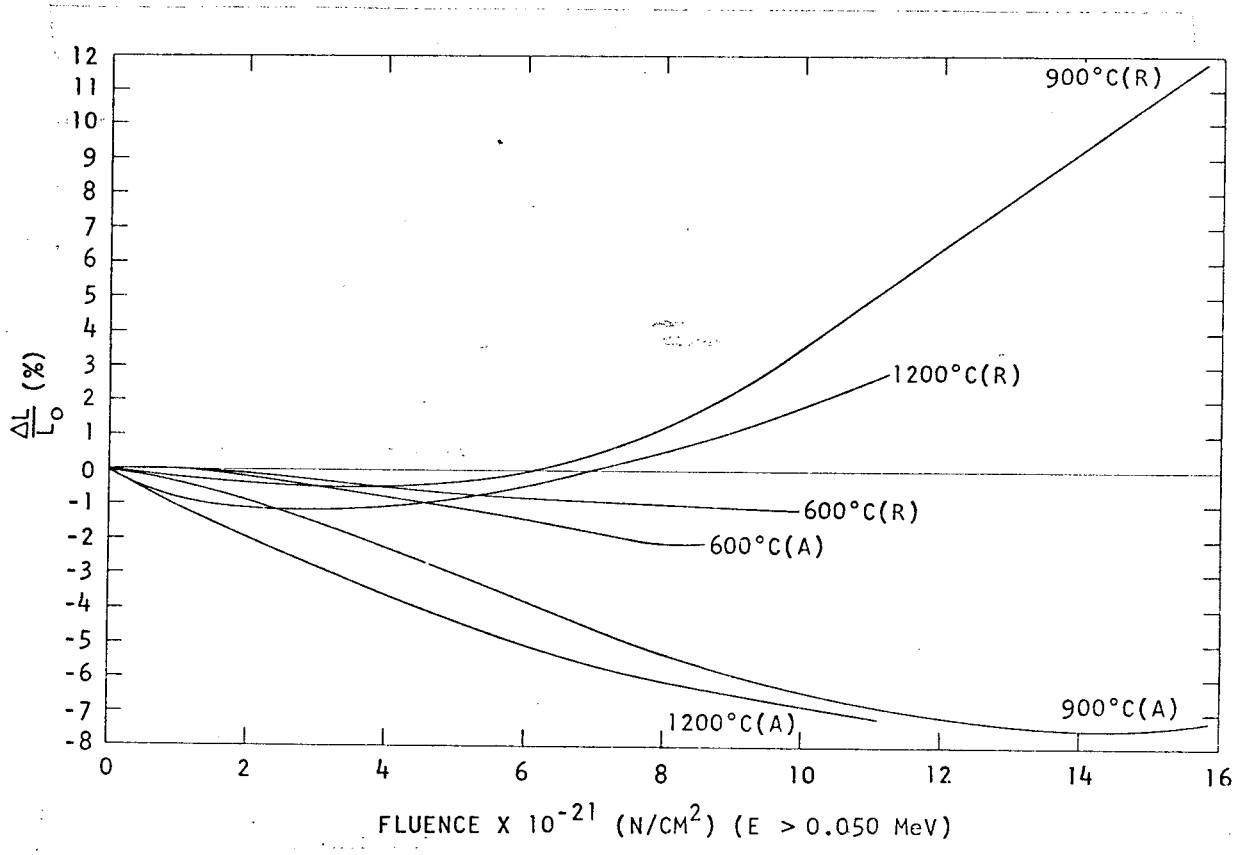

Fig. 3. Dimensional changes versus fluence of anisotropic graphites (c) Hankart et al. (September 1971)

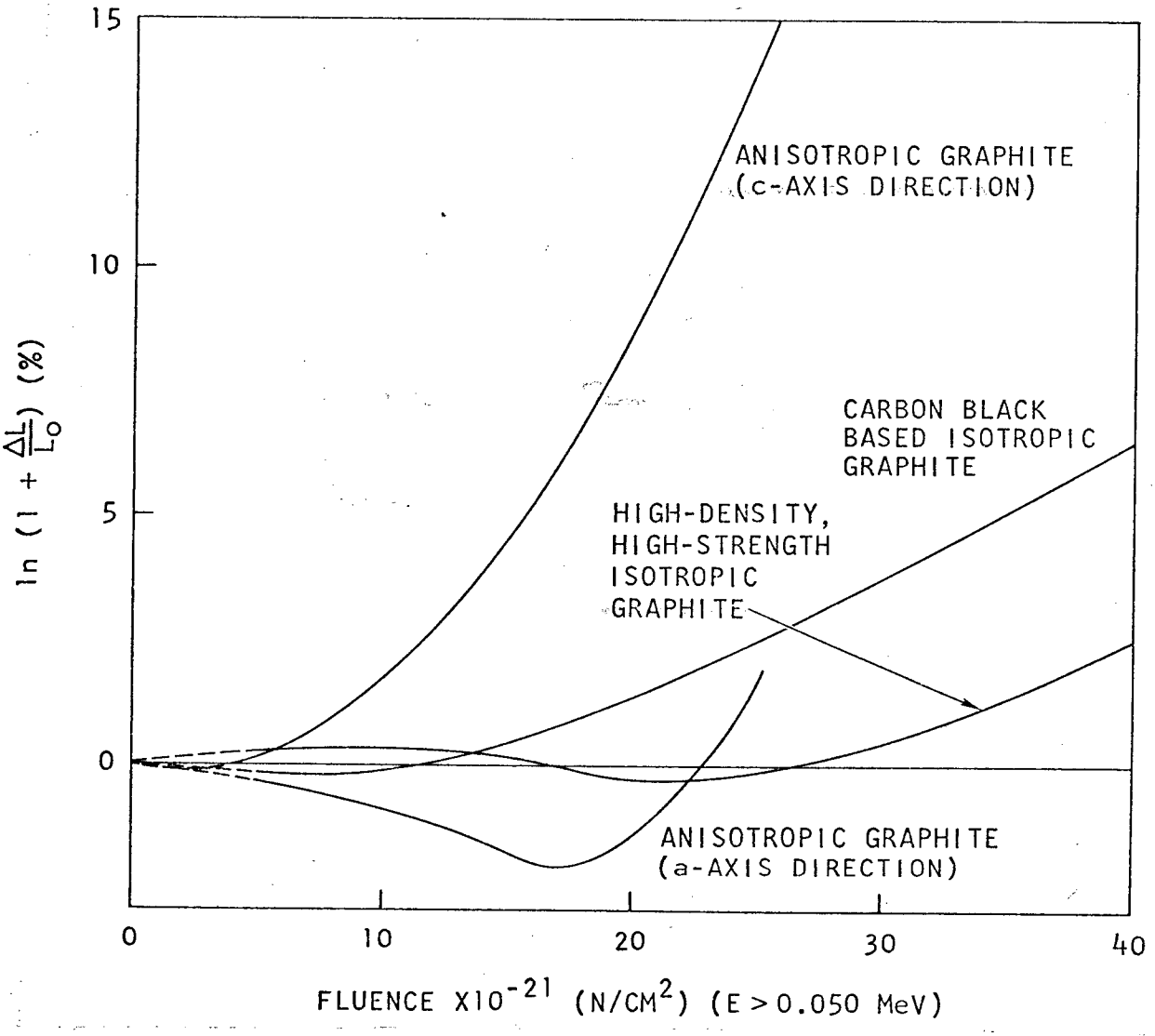

Fig. 4. Dimensional changes versus fluence of reactor graphites (Eatherly and Kennedy, 1971)

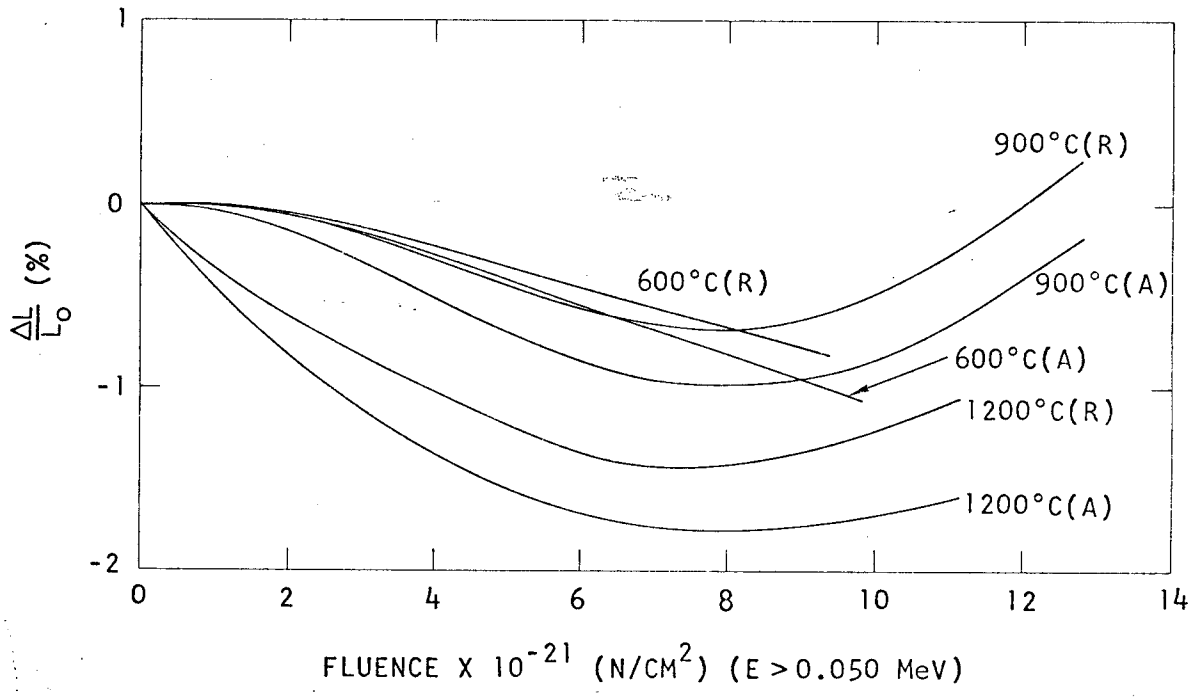

Fig. 5. Dimensional changes versus fluence of near-isotropic Gilsocoke graphites (a) Hankart et al. (September 1971)

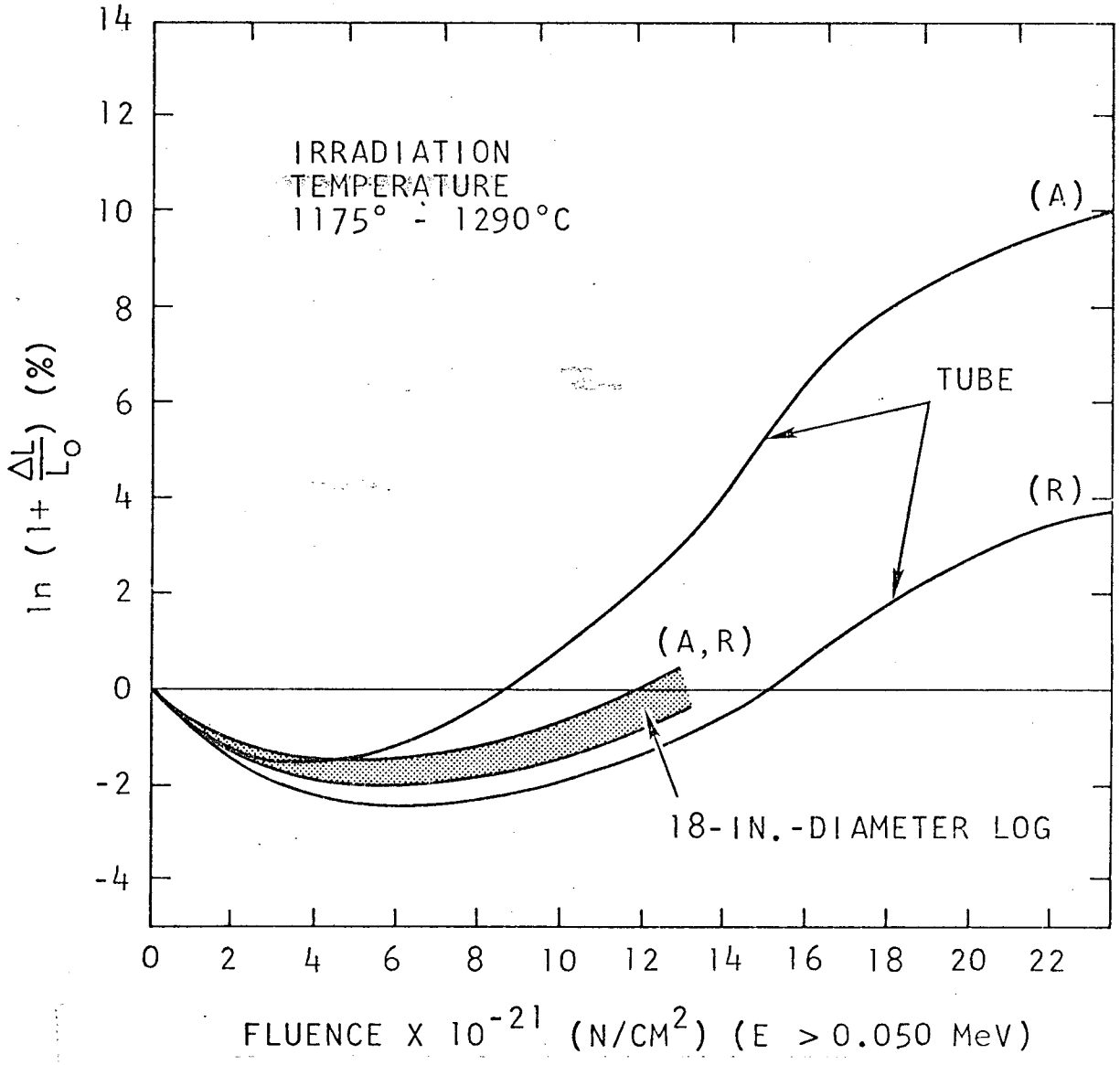

Fig. 5. Dimensional changes versus fluence of near-isotropic Gilsocoke graphites (b) Engle and Bokros (1971)

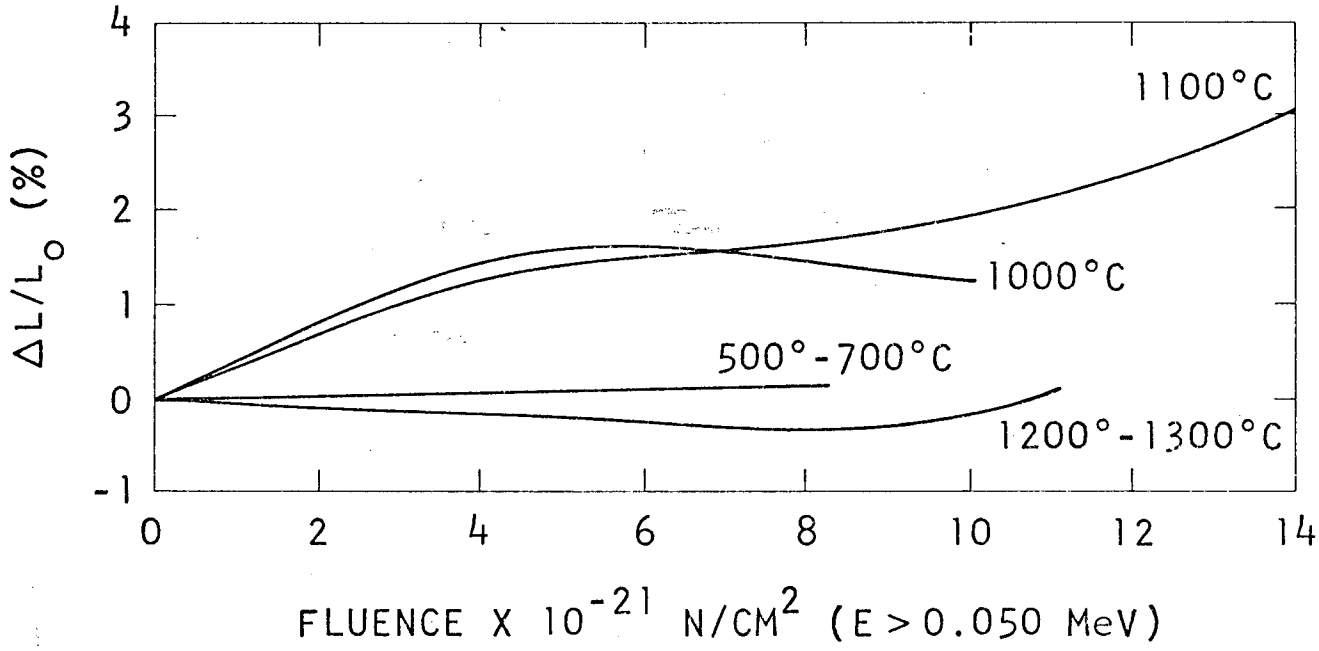

Fig. 6. Dimensional changes versus fluence of high-density, fine-grained isotropic graphites (Pitner, 1971)

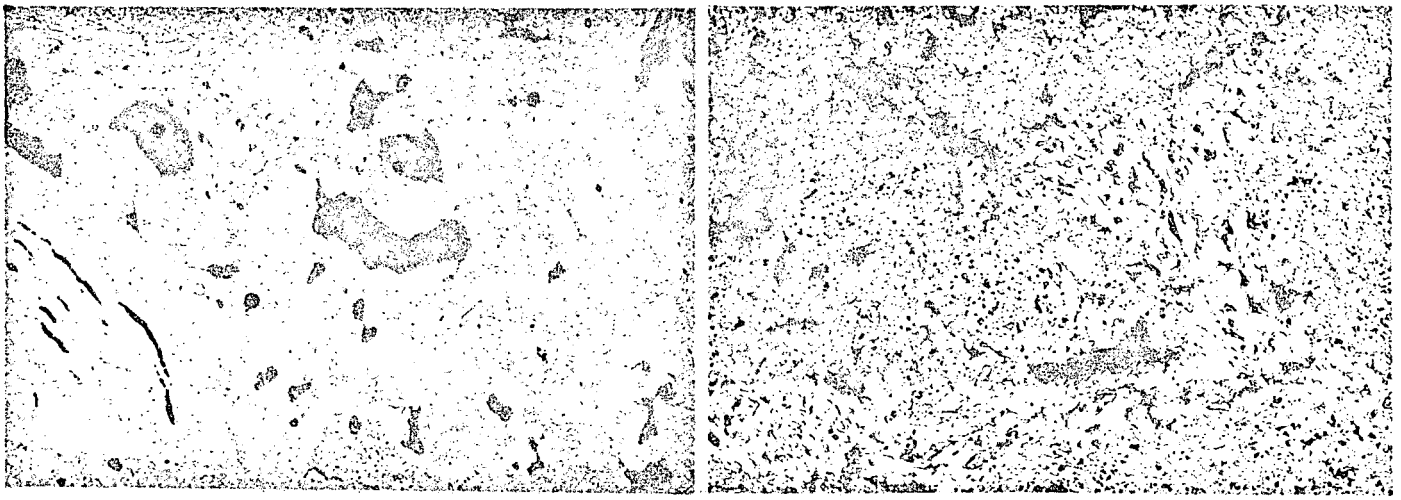

(a) (b)

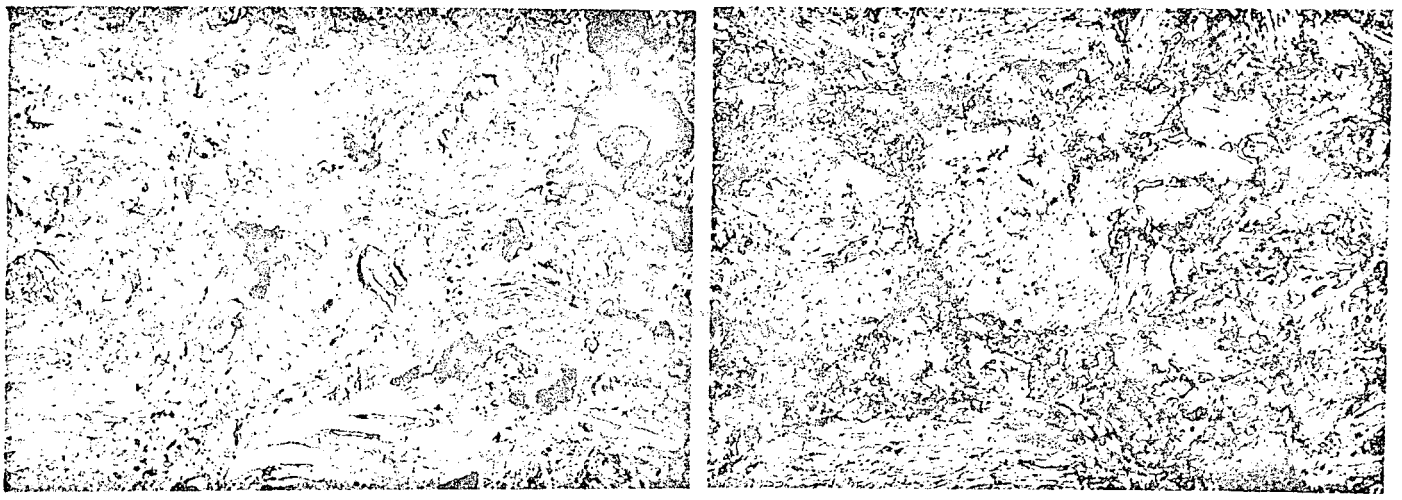

(c) (d)

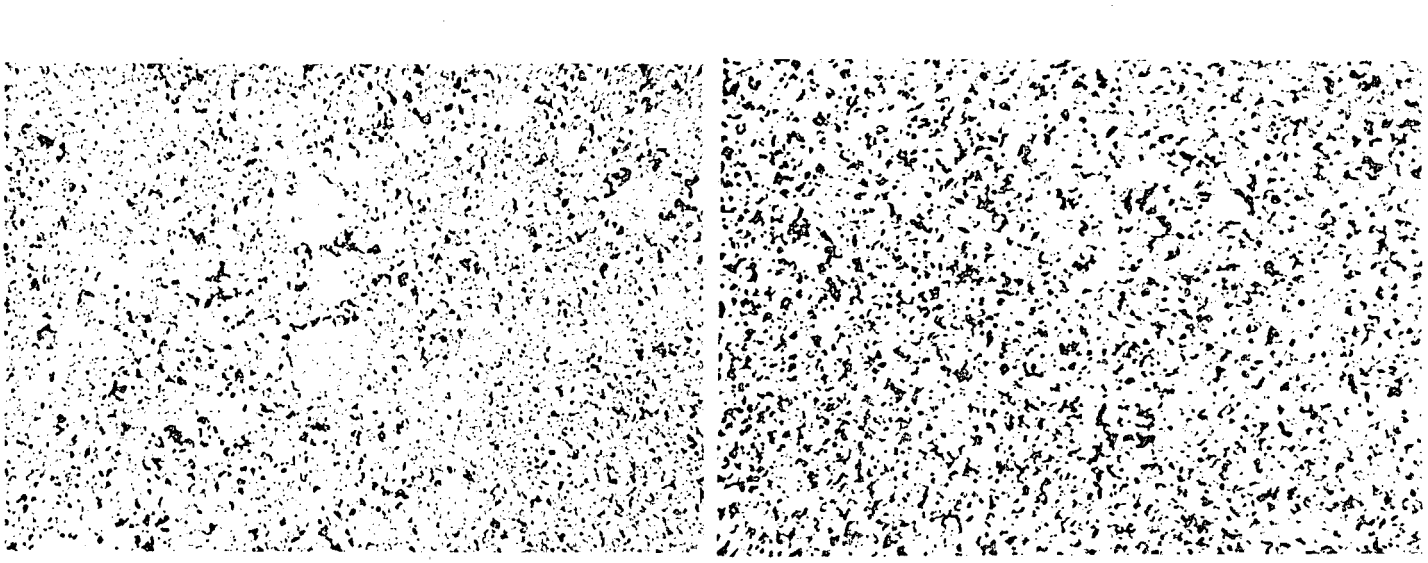

(e) (f)

Fig. 7. Photomicrographs of unirradiated and irradiated graphites.
(a) Needle coke, unirradiated, (b) Needle coke, irradiated,
(c) Gilsocoke, unirradiated, (d) Gilsocoke, irradiated,
(e) Poco graphite, unirradiated, (f) Poco graphite, irradiated

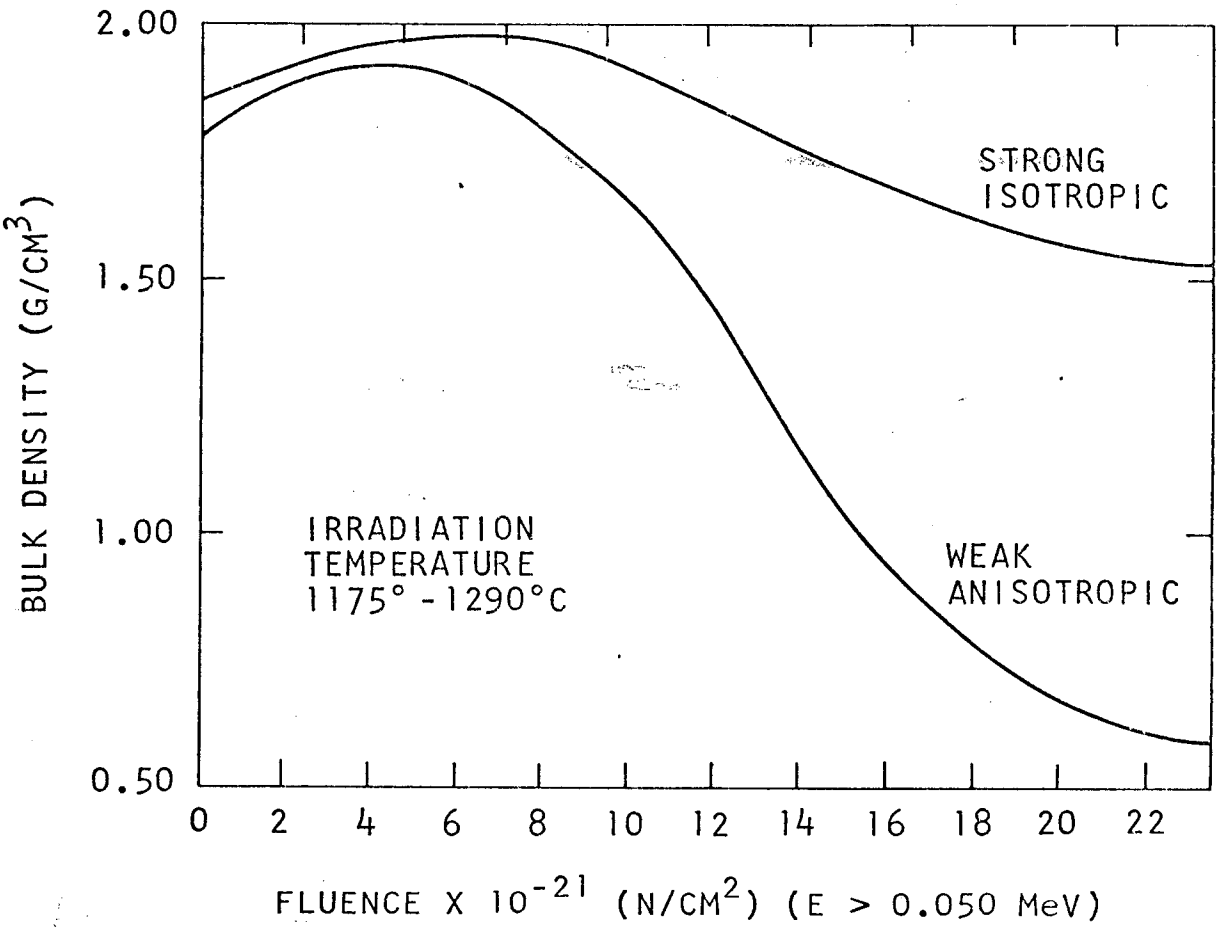

Fig. 8. Density changes in isotropic and anisotropic graphites (a) bulk density

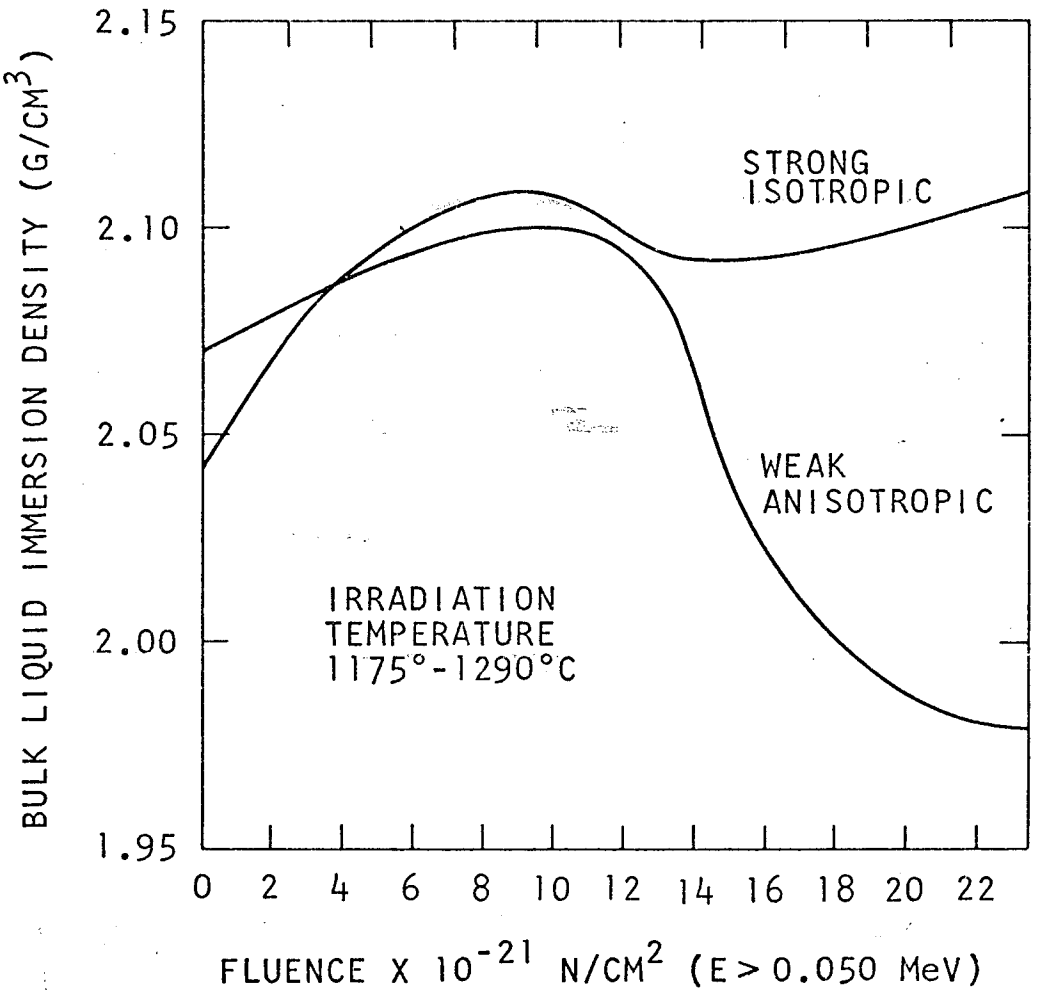

Fig. 8. Density changes in isotroipc and anisotropic graphites (b) bulk liquid by immersion density

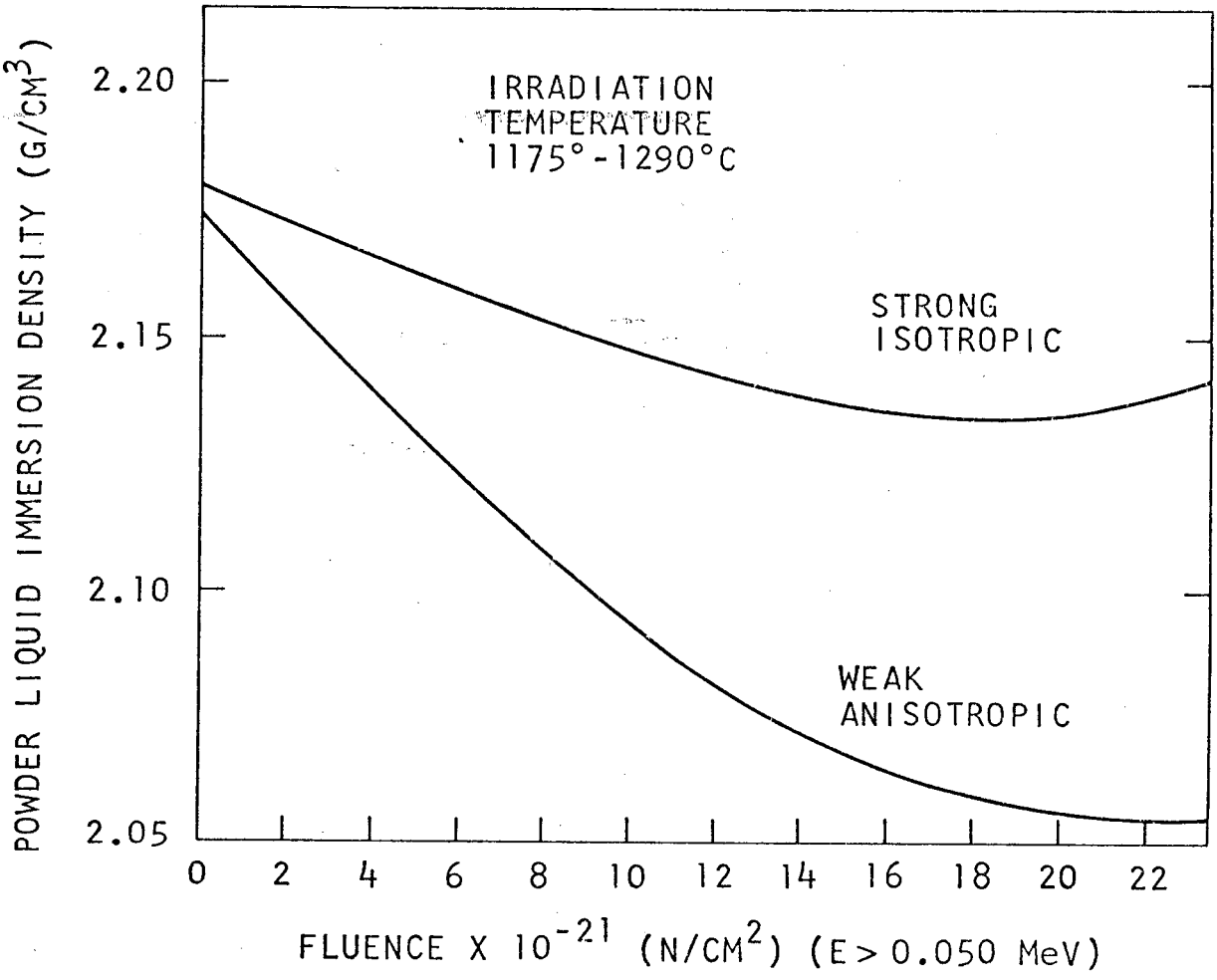

Fig. 8. Density changes in isotropic and anisotropic graphites (c) powder density by liquid immersion density

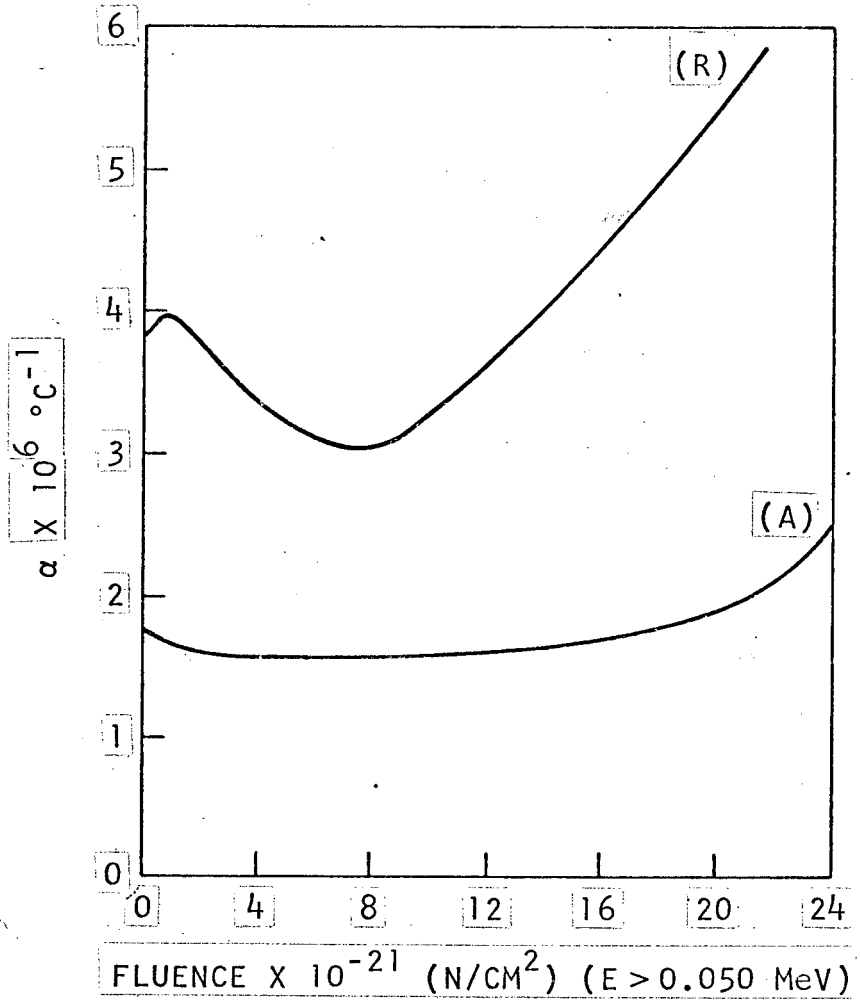

Fig. 9. Thermal expansivity versus neutron fluence of reactor graphites (a) 1000° to 1200°C (Helm, 1969)

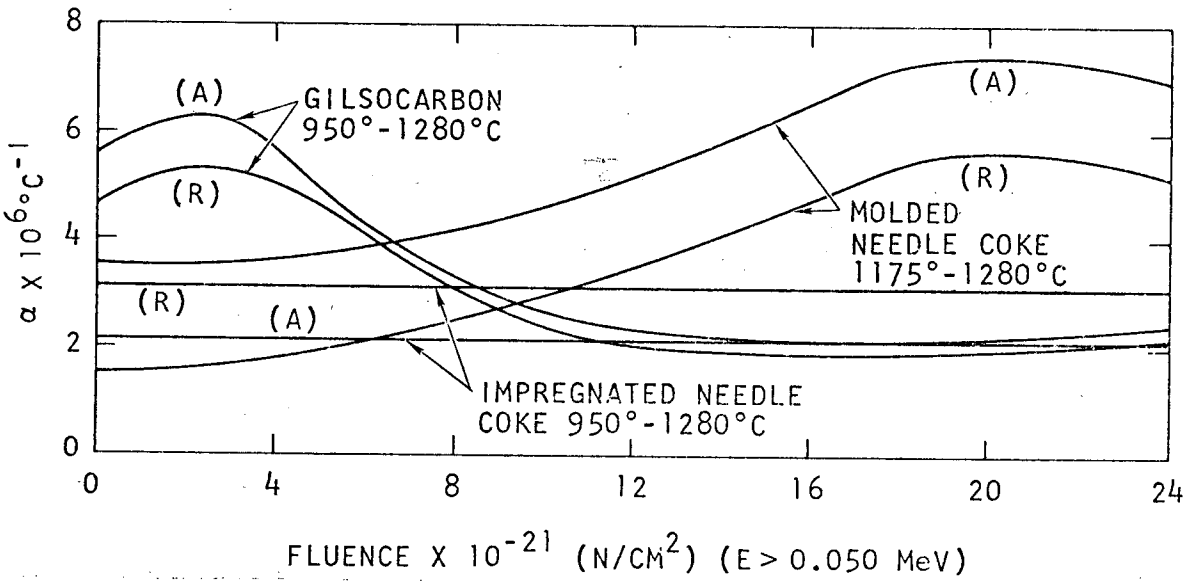

Fig. 9. Thermal expansivity versus neutron fluence of reactor graphites (b) needle coke and Gilsocoke graphites, 950° to 1280°C (Engle, August 1971)

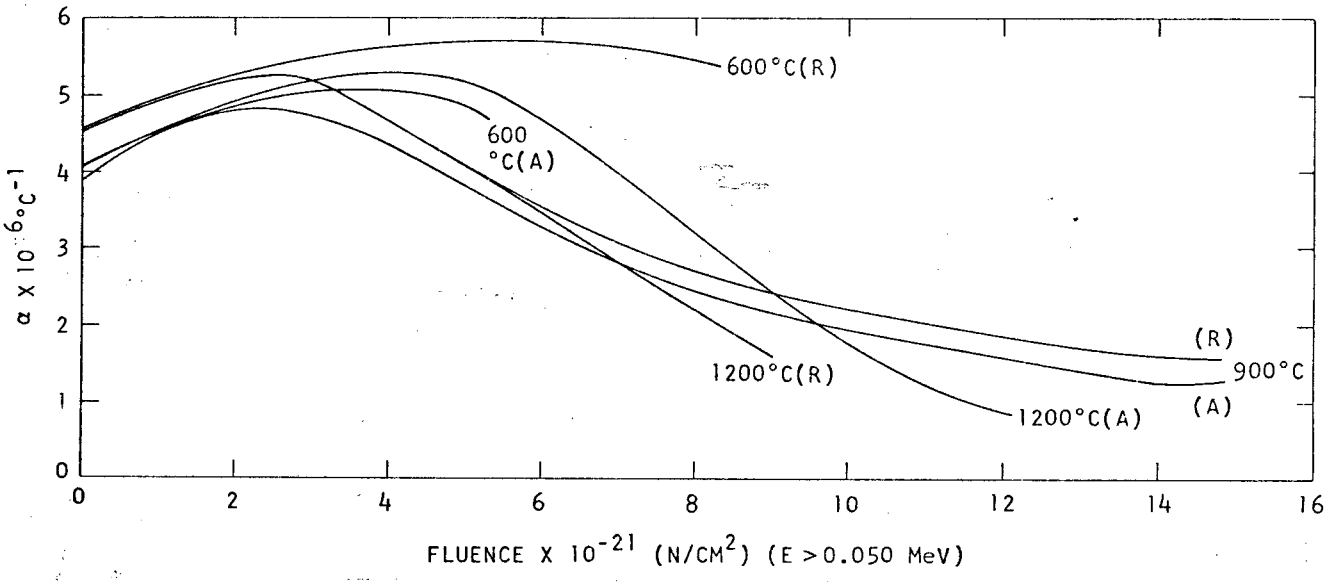

Fig. 9. Thermal expansivity versus neutron fluence of reactor graphites (c) Gilsonite graphites, 600° to 1200°C (Hankart et al., June 1971)

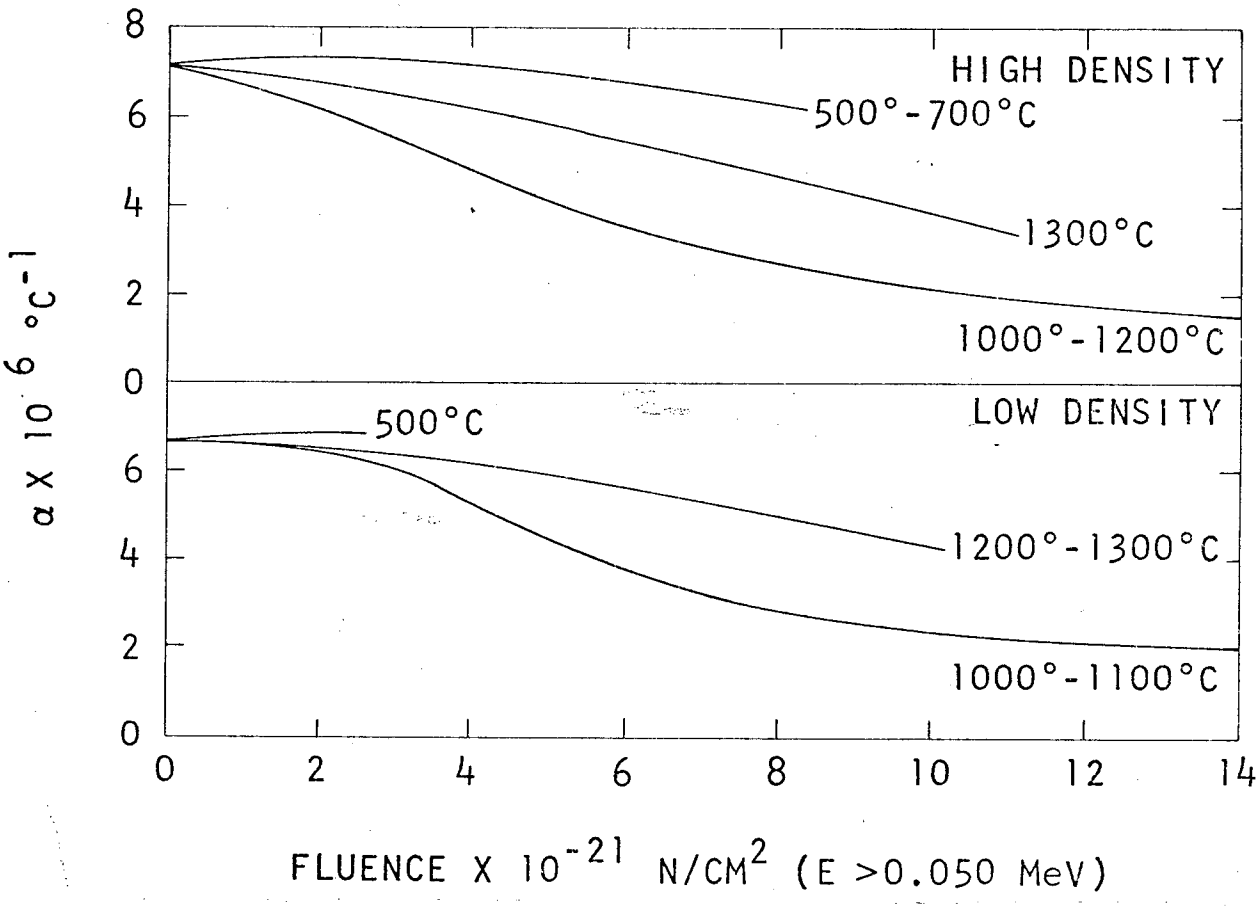

Fig. 9. Thermal expansivity versus neutron fluence of reactor graphites (d) isotropic graphites, 500° to 1300°C (Pitner, October 1971)

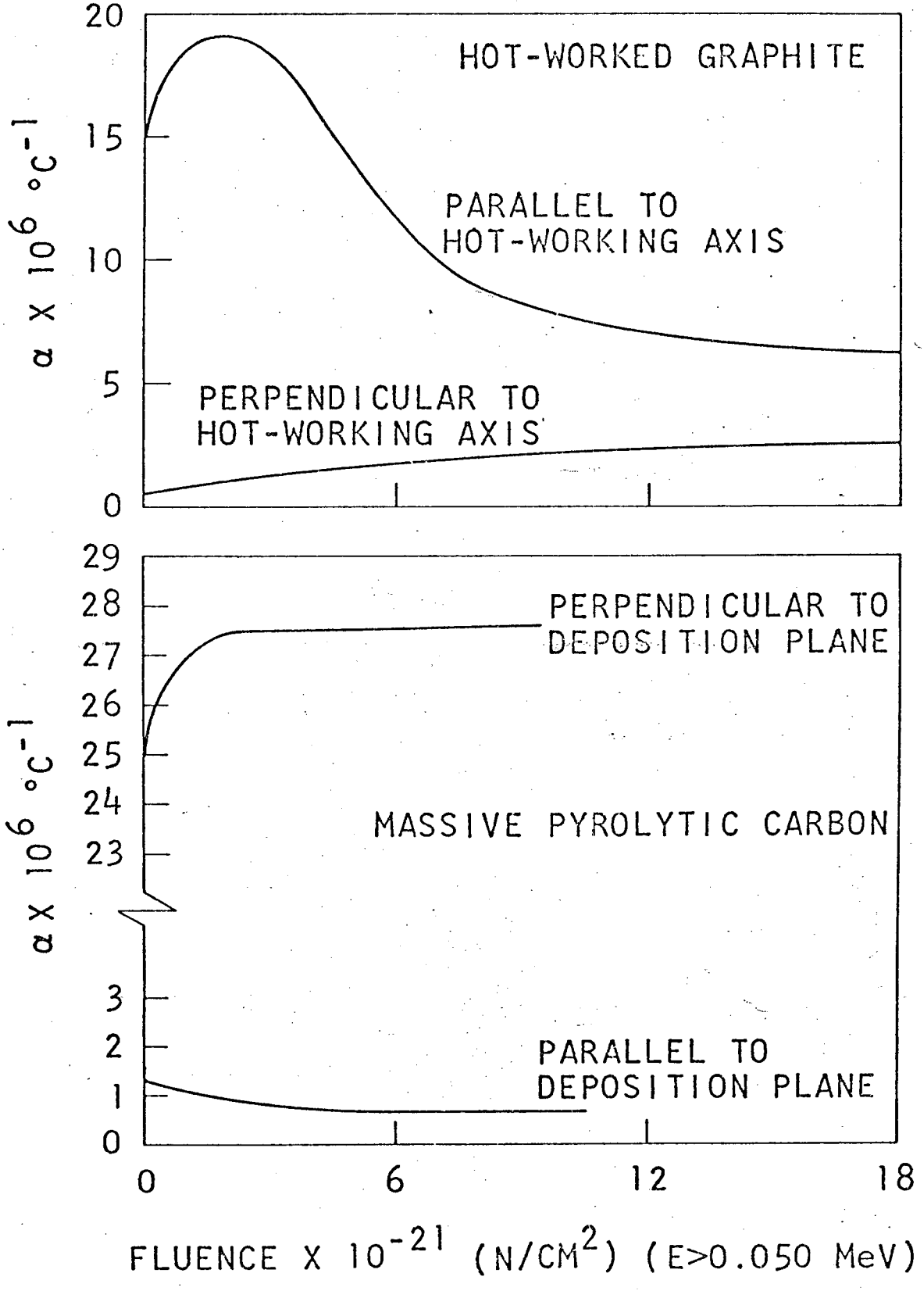

Fig. 10. Thermal expansivity in hot-worked graphite and massive pyrolytic carbon at 1250 C (Price, 1969)

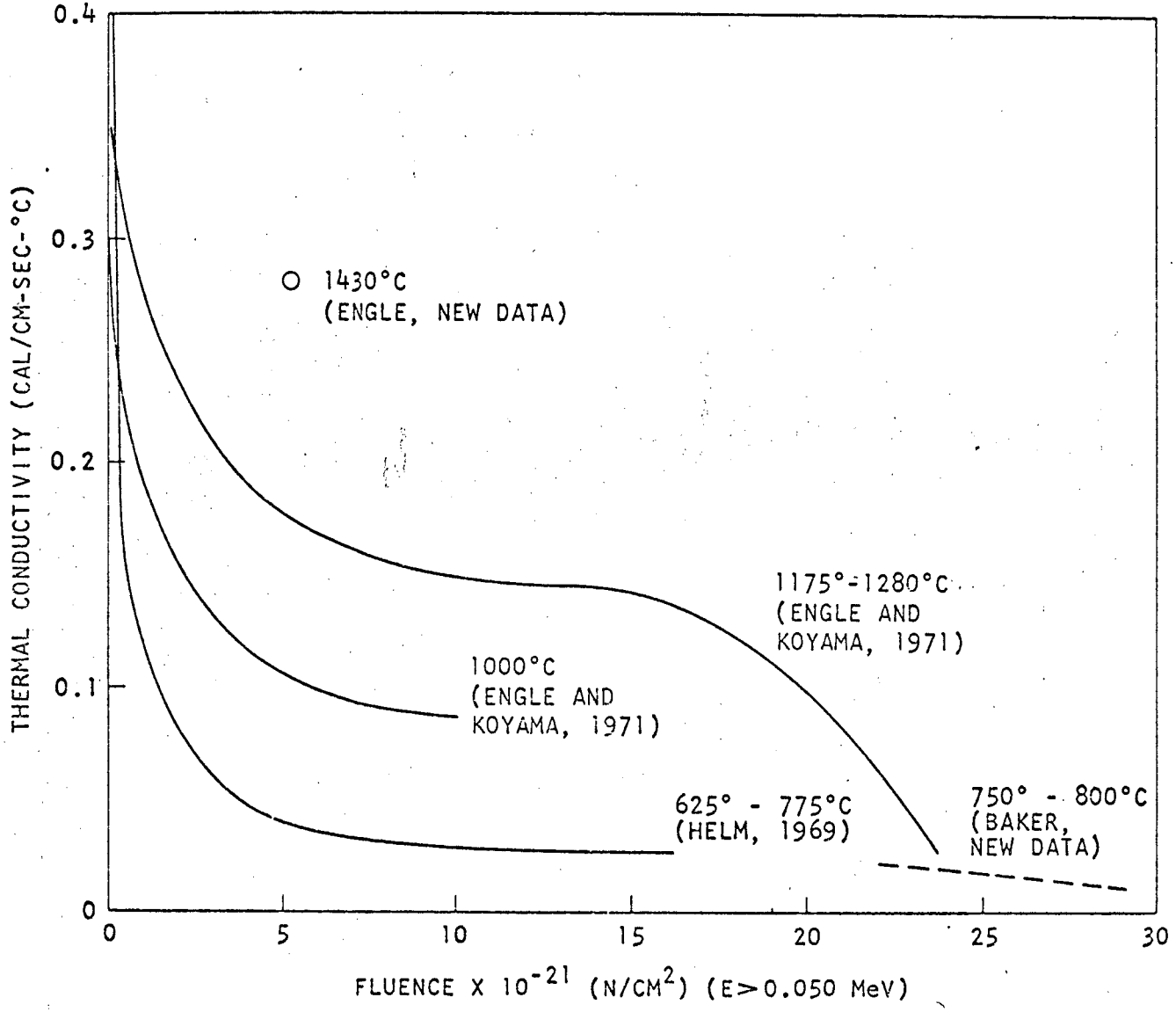

Fig. 11. Thermal conductivity changes versus fluence of reactor graphites at room temperature (Helm, 1969; Engle and Koyama, 1971)

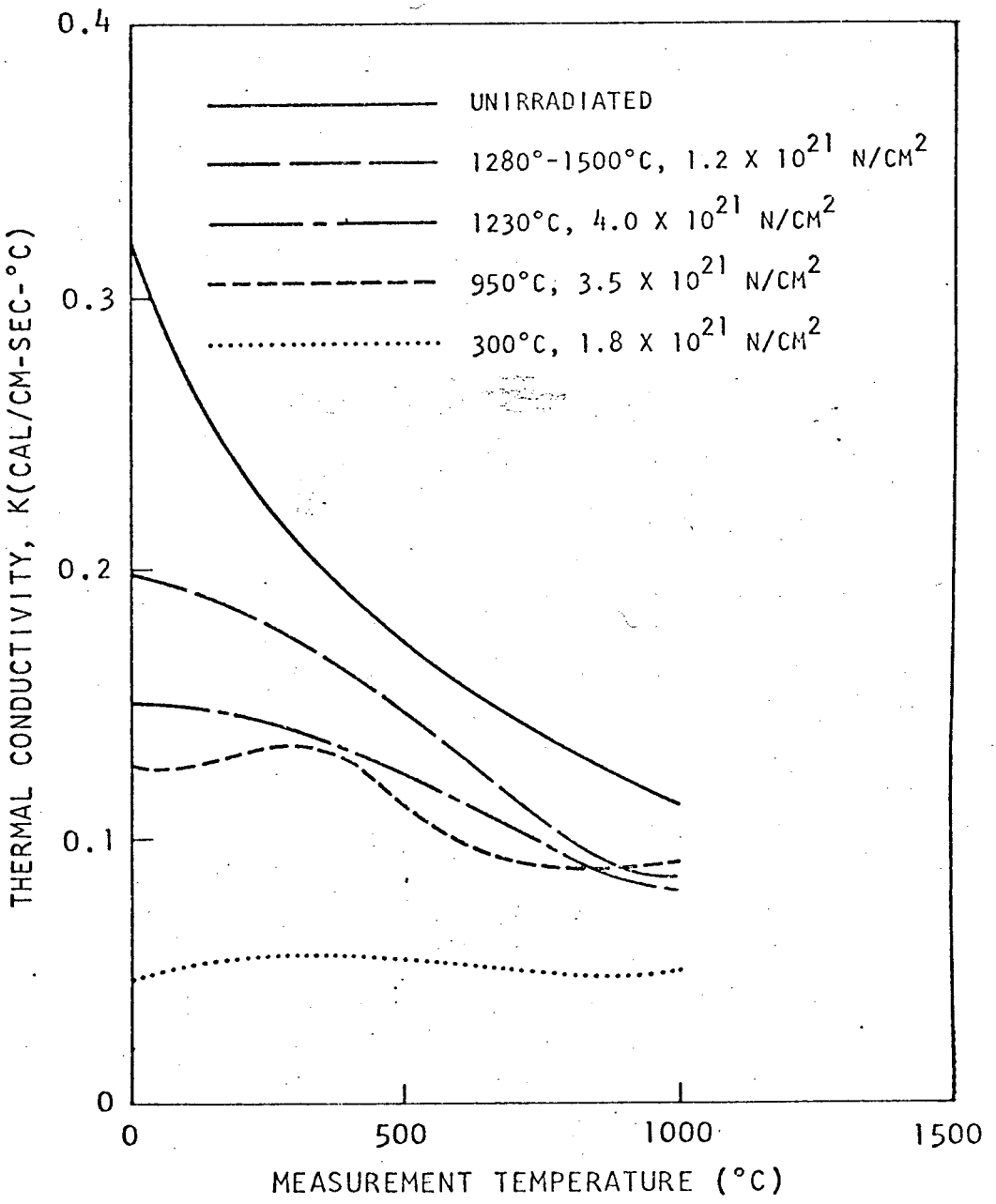

Fig. 12. Thermal conductivity changes of irradiated graphites measured at the irradiation temperature (Engle and Koyama, 1968)

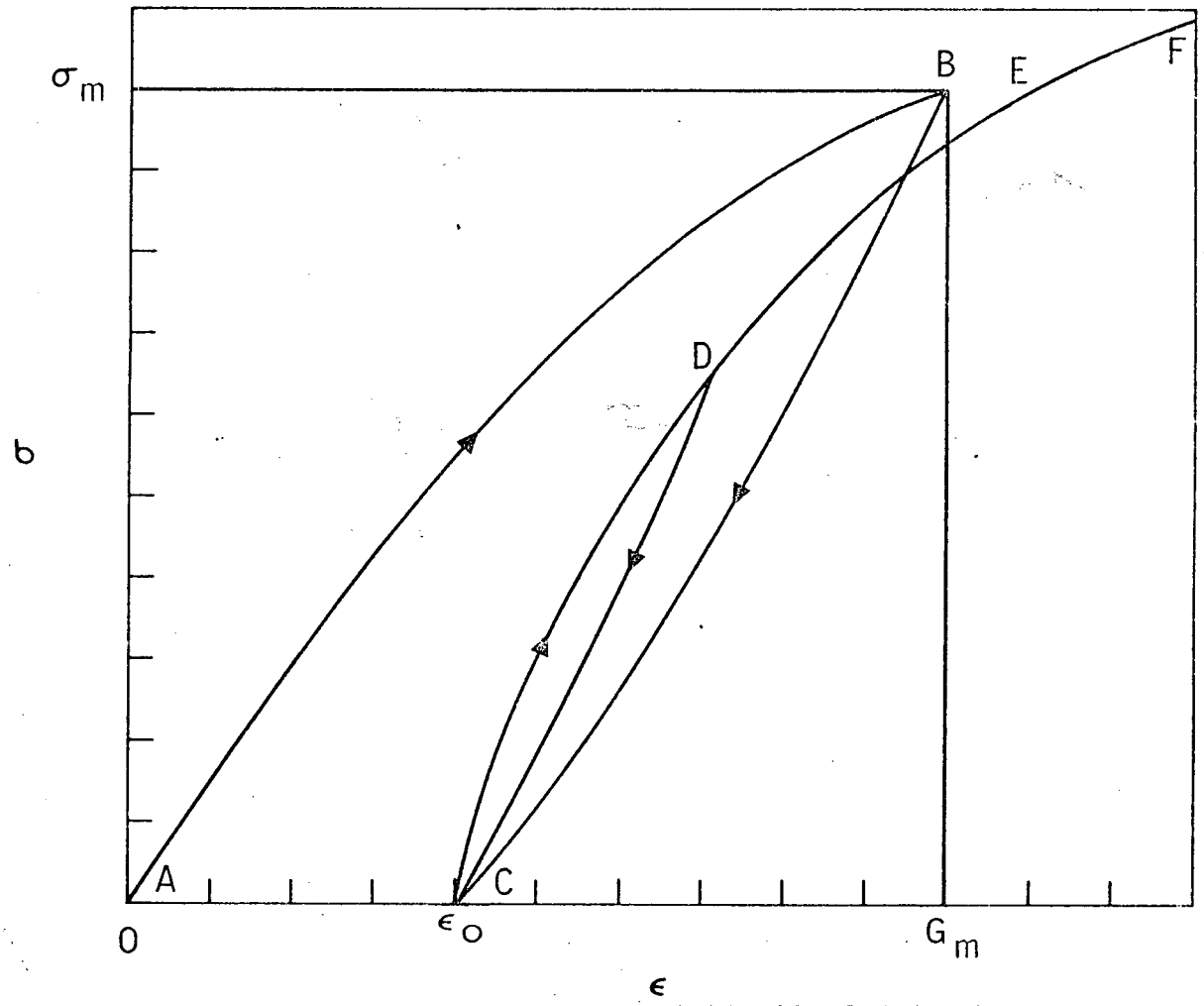

Fig. 13. Stress-strain diagram for unirradiated graphite

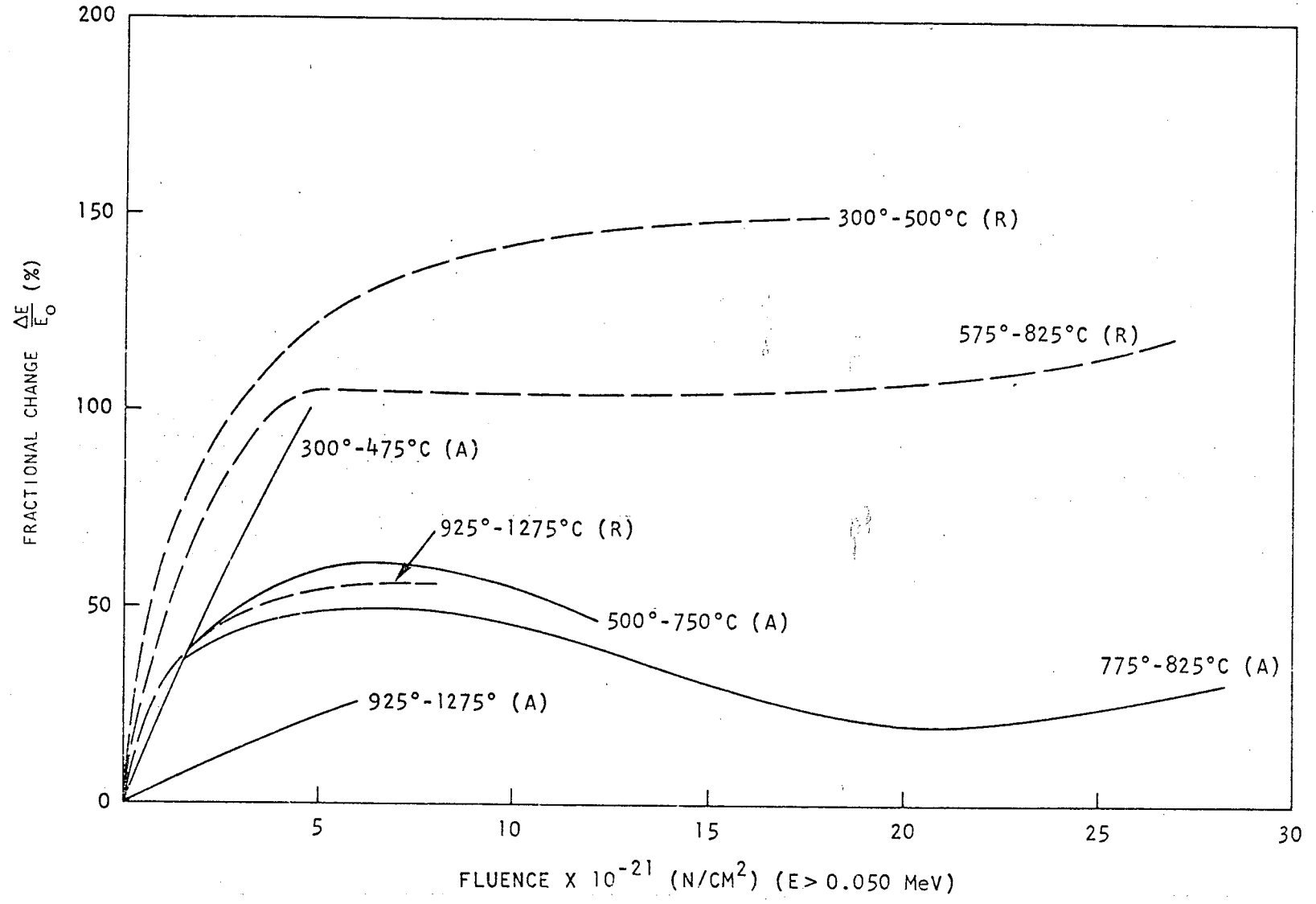

Fig. 14. Fractional change of Young's modulus $\Delta E/E$, versus fluence of an anisotropic reactor graphite. Original E values: A = 11.0×10^{10} dynes/cm^2 R = 4.8×10^{10} dynes/cm^2 (Helm, 1969)

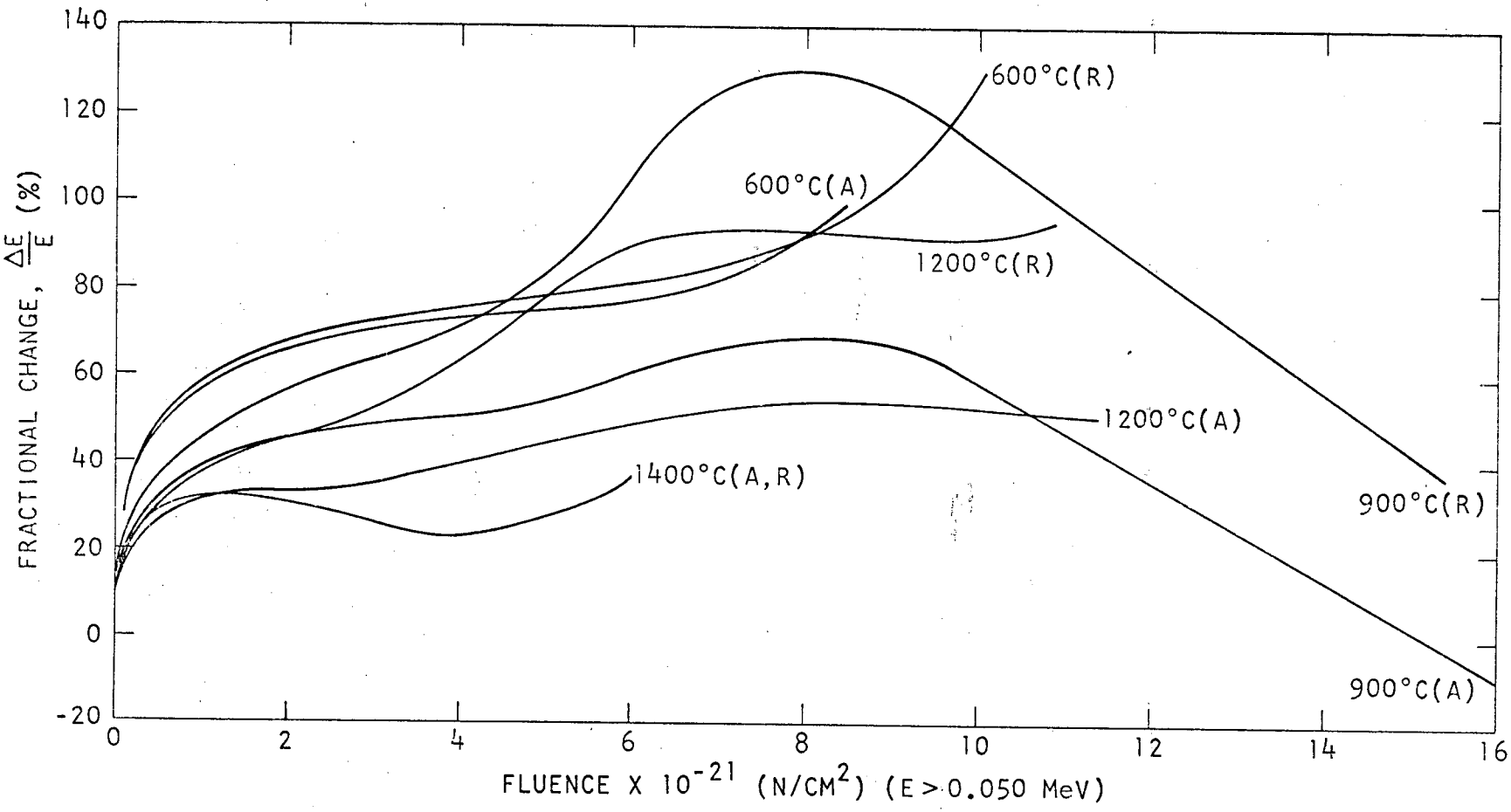

Fig. 15. Fractional change of Young's modulus, $\Delta E/E$, versus fluence for extruded experimental acicular-coke graphites. Original E values: A = 10.7 x 10^{10} dynes/cm^2, R = 6.2 x 10^{10} dynes/cm^2

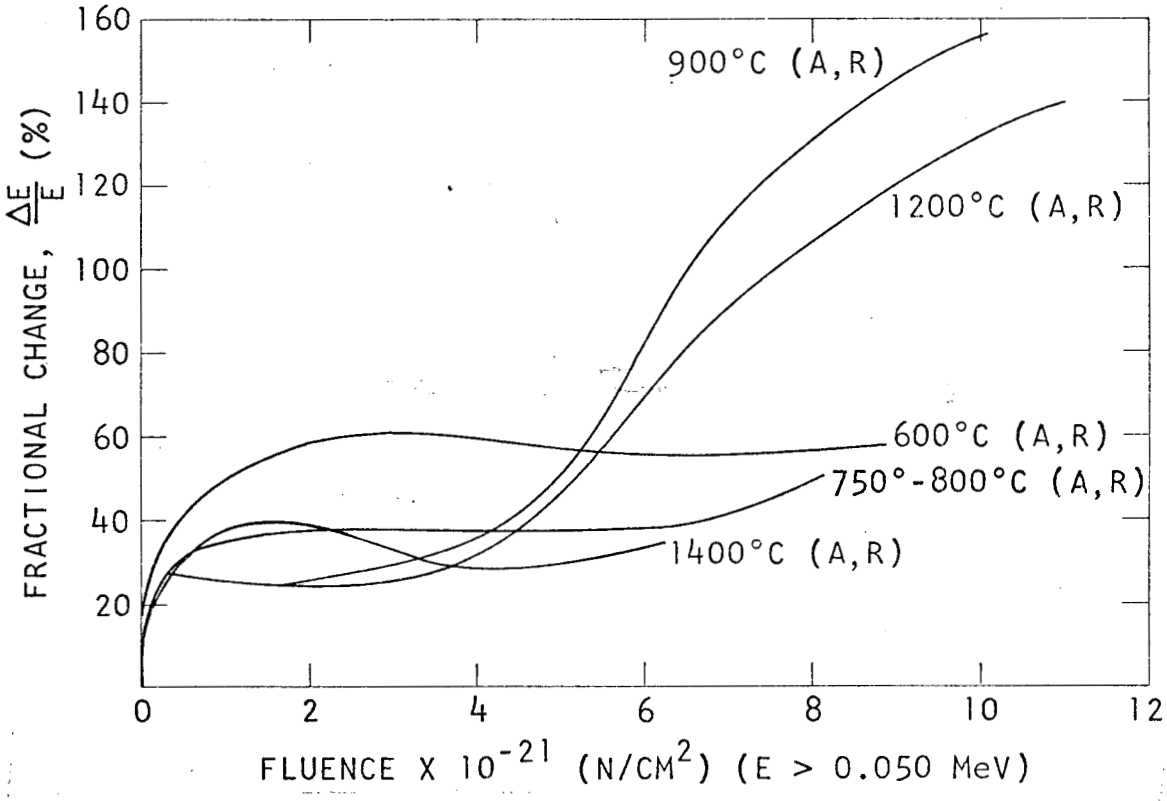

Fig. 16. Fractional change of Young's modulus, $\Delta E/E$, versus fluence for molded Gilsocoke graphites. Original E values: A = 11.9 x 10^{10} dynes/cm^2, R = 12.0 x 10^{10} dynes/cm^2

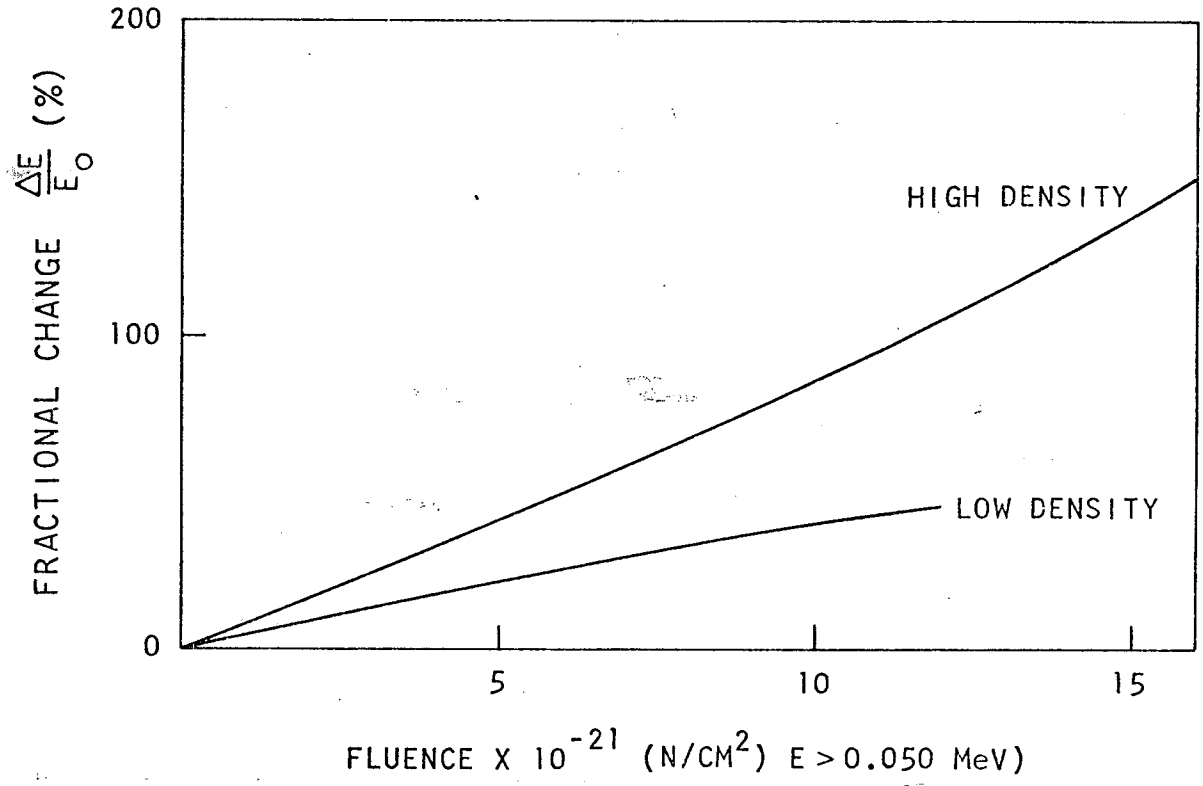

Fig. 17. Fractional change of Young's modulus, $\Delta E/E$, versus fluence for isotropic graphites. Original E values: low-density = 7.6×10^{10} dynes/cm^2, high-density = 10.4×10^{10} dynes/cm^2

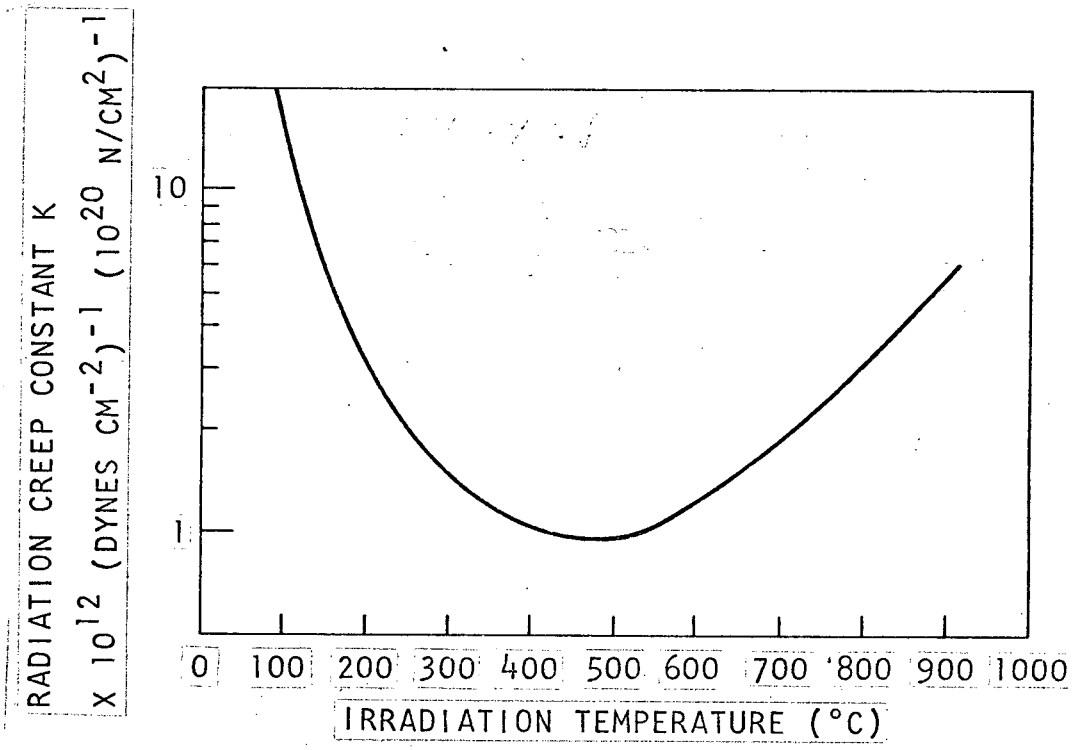

Fig. 18. Secondary creep coefficient versus temperature for irradiated graphites